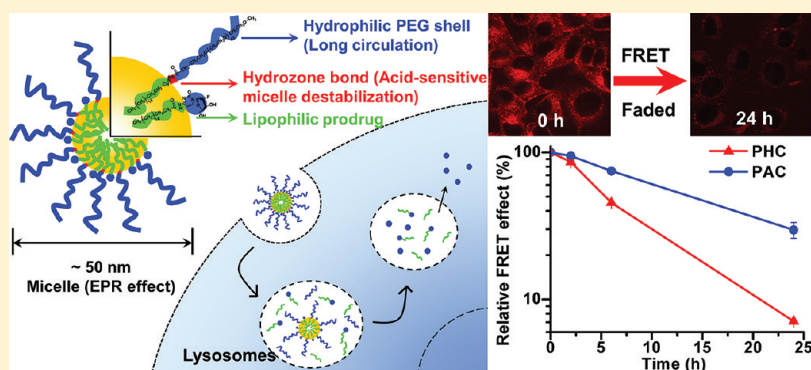


## Lysosomal Delivery of a Lipophilic Gemcitabine Prodrug Using Novel Acid-Sensitive Micelles Improved Its Antitumor Activity

Sajjie Zhu, Dharmika S. P. Lansakara-P., Xinran Li, and Zhengrong Cui\*

College of Pharmacy, Pharmaceutics Division, The University of Texas at Austin, Austin, Texas, 78712, United States

### Supporting Information



**ABSTRACT:** Stimulus-sensitive micelles are attractive anticancer drug delivery systems. Herein, we reported a novel strategy to engineer acid-sensitive micelles using an amphiphilic material synthesized by directly conjugating the hydrophilic poly(ethylene glycol) (PEG) with a hydrophobic stearic acid derivative (C18) using an acid-sensitive hydrazone bond (PHC). An acid-insensitive PEG-amide-C18 (PAC) compound was also synthesized as a control. 4-(*N*)-Stearoyl gemcitabine (GemC18), a prodrug of the nucleoside analogue gemcitabine, was loaded into the micelles, and they were found to be significantly more cytotoxic to tumor cells than GemC18 solution, likely due to the lysosomal delivery of GemC18 by micelles. Moreover, GemC18 in the acid-sensitive PHC micelles was more cytotoxic than in the acid-insensitive PAC micelles, which may be attributed to the acid-sensitive release of GemC18 from the PHC micelles in lysosomes. In B16–F10 melanoma-bearing mice, GemC18-loaded PHC or PAC micelles showed stronger antitumor activity than GemC18 or gemcitabine solution, likely because of the prolonged circulation time and increased tumor accumulation of the GemC18 by the micelles. Importantly, the *in vivo* antitumor activity of GemC18-loaded PHC micelles was significantly stronger than that of the PAC micelles, demonstrating the potential of the novel acid-sensitive micelles as an anticancer drug delivery system.

### INTRODUCTION

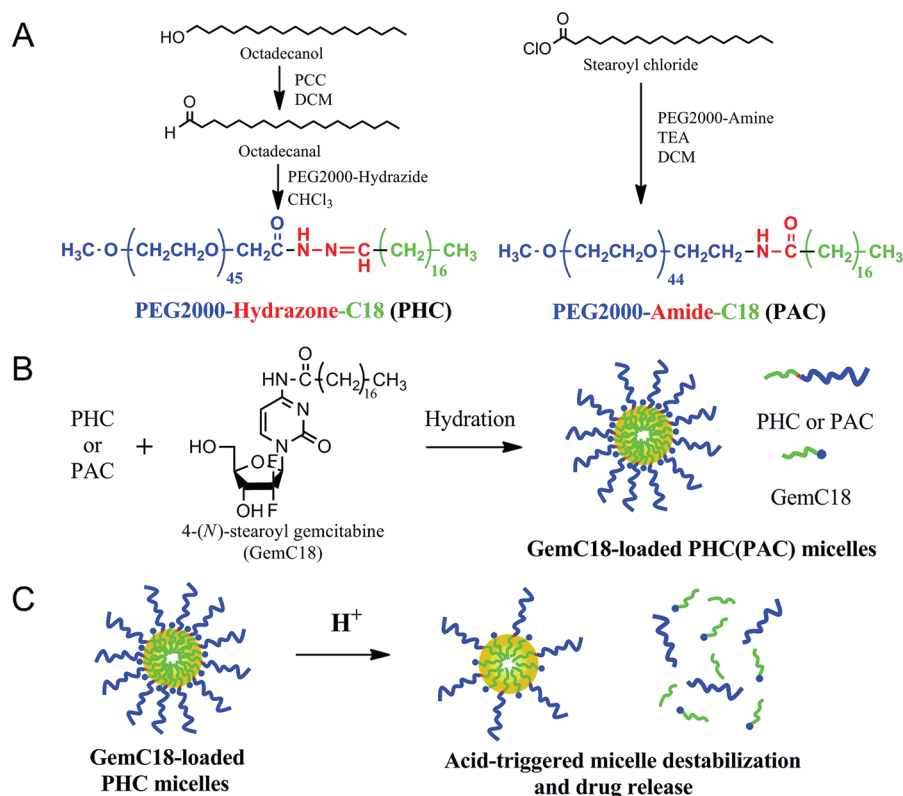
The last several decades have witnessed great progress in cancer chemotherapy, specifically the development of nanoparticulates as delivery systems for anticancer drugs, which have become increasingly attractive to researchers because of their ability to efficiently accumulate in tumors by the enhanced permeability and retention (EPR) effect.<sup>1,2</sup> Among the nanoparticulate drug delivery systems, micelles that are self-assembled from amphiphilic molecules provide a core–shell architecture, wherein the hydrophobic core serves as a natural carrier environment for hydrophobic drugs, and the hydrophilic shell allows particle stabilization in aqueous solution.<sup>3–5</sup> Micelle drug delivery systems have several documented advantages, such as ease of preparation, small and uniform particle size (10–100 nm), high drug loading, and controllable drug release profiles.<sup>6–8</sup> In addition, due to their unique structure, micelles are characteristic of hydrophilic corona, mostly composed of poly(ethylene glycol) (PEG), which create a highly water-bound barrier, block the adhesion of opsonins, and prolong the blood circulation time of micelles.<sup>9</sup>

Recently, stimulus-sensitive drug release strategies have been frequently utilized in the design of micelle drug delivery systems.<sup>10</sup> Among these stimuli, changes in acidity are particularly useful for treating solid tumors, because tumor tissues have a relatively acidic extracellular environment (pH ~6.8), compared with surrounding normal tissues. In addition, more acidic conditions (pH 5–6) are also encountered in endosomes and lysosomes once the micelles enter cells via endocytosis.<sup>11,12</sup> There are several general approaches to construct acid-sensitive micelles. One approach relies on the hydrophobic-to-hydrophilic transition of the hydrophobic segment in slightly acidic condition, which results in the destabilization of micelles and the release of drug.<sup>13,14</sup> Another approach is to covalently conjugate drug to the hydrophobic segment using acid-sensitive chemical bonds (such as hydrazone).<sup>11,15</sup> Finally, some researchers incorporate acid-

Received: November 7, 2011

Revised: March 9, 2012

Published: April 4, 2012

Scheme 1. Schematic Reaction Process and Micelle Formation<sup>a</sup>

<sup>a</sup>(A) Schemes of the synthesis of PHC and PAC conjugates. (B) Illustration of the preparation of GemC18-loaded micelles. (C) Schematic illustration of the acid-sensitive release of GemC18 from PHC micelles.

sensitive bonds into the hydrophobic polymer block, and drug release is expected when the micelles dissociate in acidic condition due to the degradation of the hydrophobic segment.<sup>16</sup> In the present study, we introduced a simple yet novel strategy for the construction of acid-sensitive micelles, by directly conjugating the hydrophilic PEG segment to a hydrophobic stearic acid derivative with an acid-sensitive hydrazone bond (Scheme 1A). The hydrolysis of the hydrazone bond in acidic condition is expected (Scheme 1B,C).

Gemcitabine (2',2'-difluoro-2'-deoxycytidine) is a deoxycytidine nucleoside analogue, which is approved for the treatment of pancreatic, non-small cell lung, breast, and ovarian cancers.<sup>17</sup> Clinical trials using gemcitabine for melanoma therapy have also been reported.<sup>18,19</sup> Despite its effective anticancer activity, gemcitabine suffers from various drawbacks, such as rapid deamination to inactive 2',2'-difluorodeoxyuridine (dFdU) by cytidine deaminase after intravenous (i.v.) injection, resulting in a short *in vivo* half-life (8–17 min).<sup>20</sup> A lipophilic prodrug strategy has been explored by conjugating gemcitabine with a long fatty acid chain, which was shown to prevent the deamination.<sup>21</sup> In addition, it is relatively easier to load the lipophilized gemcitabine into lipid-based nanoparticulate drug delivery systems, as compared with the highly hydrophilic gemcitabine.<sup>22,23</sup> For example, Couvreur's group covalently coupled gemcitabine with 1,1',2-tris-*nor*-squalenic acid and formulated the resultant 4-(*N*)-tris-*nor*-squalenoyl-gemcitabine (SQdFdC) into nanoparticles,<sup>24,25</sup> which were shown to increase the survival of mice with murine metastatic leukemia (L1210 wt), as compared with gemcitabine alone. Similarly, 4-(*N*)-stearoyl-gemcitabine (GemC18), a stearic acid amide derivative of gemcitabine,<sup>21</sup> also showed improved antitumor

activity in mouse models when delivered using liposomes or solid lipid nanoparticles, again as compared with gemcitabine alone.<sup>21,23</sup>

In the present study, the feasibility of using the novel acid-sensitive micelles as a carrier for the gemcitabine prodrug, GemC18, was evaluated both *in vitro* and *in vivo*. Furthermore, a lipophilic fluorescence resonance energy transfer (FRET) pair was incorporated into the micelles to confirm the acid-sensitivity of the micelles at the cellular level, and the significance of the lysosomal delivery of the amide prodrug, GemC18, was discussed accordingly.

## EXPERIMENTAL PROCEDURES

**Materials.** Gemcitabine hydrochloride (GemHCl) was from U. S. Pharmacopeia (Rockville, MD). Methoxy-poly(ethylene glycol) 2000-hydrazide (PEG2000-hydrazide) and methoxy-poly(ethylene glycol) 2000-amine (PEG2000-amine) were from Creative PEGWorks (Wiston Salem, NC). Pyridinium chlorochromate (PCC) and pyrene were from Acros Organics (Morris Plains, NJ). 1-Hydroxy-7-azabenzotriazole (HOAt) was from CreoSalus, Inc. (Louisville, KY). Octadecanol, stearoyl chloride, stearic acid, sodium dodecyl sulfate (SDS), 1-ethyl-3-(3-dimethylaminopropyl)carbodiimide (EDCI), 3-(4,5-dimethylthiazol-2-yl)-2,5-diphenyltetrazolium bromide (MTT), uracil 1- $\beta$ -D-arabinofuranoside (AraU), 1,1'-dioctadecyl-3,3',3'-tetramethylindocarbocyanine perchlorate (DiI), and 3,3'-dioctadecyloxycarbocyanine perchlorate (DiO) were from Sigma-Aldrich (St. Louis, MO). Lysotracker Red DND-99 was from Molecular Probes (Eugene, OR). Hoechst 33342 was from AnaSpec, Inc. (Fremont, CA). The *in situ* cell death detection kit, TMR red, was from Roche Diagnostics

(Indianapolis, IN). Bromodeoxyuridine (BrdU) and primary BrdU monoclonal antibody were from BD Biosciences (San Jose, CA). Biotinylated rabbit-antimouse F(ab)' was from Accurate Chem (Westbury, NY). HPLC-grade tetrahydrofuran (THF) and methanol were used during HPLC analysis, and other solvents used in chemical synthesis and cell culture work were of analytical grade. Water was purified using a Millipore filtration system (Millipore Corporation, Billerica, MA).

Murine melanoma B16-F10 cells and human pancreatic cancer BxPC-3 cells were from (American Type Culture Collection, ATCC, Manassas, VA) and grown in RPMI 1640 medium and DMEM medium, respectively. All media were supplemented with 10% fetal bovine serum (FBS), 100 U/mL of penicillin, and 100  $\mu$ g/mL of streptomycin, all from Invitrogen (Carlsbad, CA).

Proton NMR ( $^1\text{H}$  NMR) spectra were recorded using a 300 MHz Varian UNITY Plus instrument. The molecular weights of PEG derivatives were determined with a Varian 12T FTICR equipped with a Nd:YAG laser emitting at 355 nm (Varian, Inc., Palo Alto, CA) using matrix-assisted laser desorption/ionization (MALDI). For other compounds, the molecular weight was determined on a Thermo Scientific TSQ Quantum GC Triple Quad (Thermo Scientific, Pittsburgh, PA) using chemical ionization.

**Synthesis of PEG2000-hydrazone-C18 (PHC). Synthesis of octadecanal.** The synthetic procedure of octadecanal was adapted from Easton et al.<sup>26</sup> Briefly, PCC (600.0 mg, 2.78 mmol) was suspended in dichloromethane (DCM) (6 mL), and octadecanol (600.0 mg, 2.22 mmol) in DCM (12 mL) was then rapidly added at room temperature. The reaction was kept at room temperature for 2 h with magnetic stirring (750 rpm), after which diethyl ether ( $\text{Et}_2\text{O}$ ) (36 mL) was added to the reaction mixture. Insoluble reduced reagent was removed by centrifugation, and the crude product was obtained by drying the supernatant. Final purification of the product was performed on silica gel (hexane/ $\text{Et}_2\text{O}$ , 96:4) to give octadecanal (320.0 mg, 53.7% yield) as a white solid.  $R_f$  = 0.52 (chloroform ( $\text{CHCl}_3$ )).  $^1\text{H}$  NMR (300 MHz,  $\text{CDCl}_3$ ):  $\delta$  = 9.74 (t, 1H, C(O)H), 2.39 (t, 2H,  $\text{COCH}_2$ ), 1.61 (m, 2H,  $\text{COCH}_2\text{CH}_2$ ), 1.23 (m, 28H,  $(\text{CH}_2)_{14}$ ), 0.86 ppm (t, 3H,  $\text{CH}_3$ ). MS  $[\text{M}+\text{H}]^+$   $m/z$  calculated for  $\text{C}_{18}\text{H}_{36}\text{O}$ : 268.2766, found: 268.2769. **Synthesis of PHC.** Octadecanal (100.0 mg, 0.372 mmol) was reacted with PEG2000-hydrazide (200.0 mg, 0.1 mmol) in 4.8 mL of dry  $\text{CHCl}_3$  at 50  $^\circ\text{C}$  under argon and molecular sieves. After 24 h of reaction, the mixture was concentrated with a rotary evaporator and then applied to a silica gel column. Chloroform was first used as the mobile phase to separate excessive octadecanal, after which  $\text{CHCl}_3$ /methanol (10:1) was used to collect PHC (151.3 mg, 67.6% yield) as a white solid.  $R_f$  = 0.22 ( $\text{CHCl}_3$ /methanol, 9:1).  $^1\text{H}$  NMR (300 MHz,  $\text{CDCl}_3$ ):  $\delta$  = 9.82 (t, 1H,  $\text{CONHN}=\text{CH}$ ), 7.46 (s, 1H,  $\text{N}=\text{CH}$ ), 3.5–3.7 (m, 180H,  $(\text{CH}_2\text{CH}_2\text{O})_{45}$ ), 3.36 (s, 3H,  $\text{OCH}_3$ ), 2.34 (t, 2H,  $\text{COCH}_2$ ), 1.49 (m, 2H,  $\text{COCH}_2\text{CH}_2$ ), 1.23 (m, 28H,  $(\text{CH}_2)_{14}$ ), 0.85 ppm (t, 3H,  $\text{CH}_3$ ).

**Synthesis of PEG2000-amide-C18 (PAC).** To the solution of PEG2000-amine (220 mg, 0.11 mmol) in 3 mL dry DCM, 46  $\mu\text{L}$  (0.33 mmol) of triethylamine (TEA) was added at room temperature, followed by dropwise addition of stearoyl chloride (100 mg, 0.33 mmol) in 2 mL of dry DCM. The reaction mixture was then placed on a plate of 30  $^\circ\text{C}$ , while stirring at 500 rpm. About 20 h later, the solvent was evaporated with a rotary evaporator, and the crude product was recrystallized twice with 5 mL of  $\text{Et}_2\text{O}$ . The solid obtained was

further purified with a silica gel column ( $\text{CHCl}_3$ /methanol, 4:1) to give PEG2000-amide-C18 (205.2 mg, 82.3% yield) as a white solid.  $R_f$  = 0.41 ( $\text{CHCl}_3$ /methanol, 9:1).  $^1\text{H}$  NMR (300 MHz,  $\text{CDCl}_3$ ):  $\delta$  = 6.06 (s, 1H,  $\text{NHCO}$ ), 3.5–3.7 (m, 176H,  $(\text{CH}_2\text{CH}_2\text{O})_{44}$ ), 3.36 (s, 3H,  $\text{OCH}_3$ ), 2.14 (t, 2H,  $\text{COCH}_2$ ), 1.59 (m, 2H,  $\text{COCH}_2\text{CH}_2$ ), 1.23 (m, 28H,  $(\text{CH}_2)_{14}$ ), 0.85 ppm (t, 3H,  $\text{CH}_3$ ).

**Synthesis of 4-(*N*-Stearoyl Gemcitabine (GemC18).** 4-(*N*-Stearoyl gemcitabine (GemC18) was synthesized according to literature procedures with slight modifications.<sup>23,27</sup> The primary and secondary alcohols of the deoxyribofuranose ring of gemcitabine were first Boc(*tert*-butoxycarbonyl)-protected to produce 3',5'-*O*-bis(*tert*-butoxycarbonyl) gemcitabine.<sup>27</sup> Next, Boc-protected gemcitabine (219 mg, 0.47 mmol), stearic acid (149 mg, 0.52 mmol), and HOAt (70 mg, 0.52 mmol) were dissolved in anhydrous DCM at 4  $^\circ\text{C}$ , followed by the addition of 109 mg of EDCI (0.57 mmol). After degassing by vacuum sonication, the reaction mixture was kept at room temperature for another 40 h in argon atmosphere. Water (15 mL) was added, and the mixture was extracted with ethyl acetate ( $\text{EtOAc}$ )/hexane (2:1). The organic phase was washed with saturated ammonium chloride ( $\text{NH}_4\text{Cl}$ ) and brine, dried over anhydrous  $\text{Na}_2\text{SO}_4$ , and then evaporated. The residue obtained was purified using a silica gel column ( $\text{EtOAc}$ /Hexane, 3:7) to give Boc-protected-*N*-stearoyl gemcitabine as a white powder. The obtained product (319 mg, 0.44 mmol) was then dissolved in 7 mL of DCM, followed by the addition of 1.5 mL of trifluoroacetic acid (TFA). After 2 h of stirring at room temperature, excessive TFA was removed under reduced pressure, and the concentrated sample was co-distilled with DCM 5 times. A silica gel column was used to purify this crude sample (DCM/ethanol, 94:6), and the desired product of GemC18 was obtained as a white powder (162 mg, 64.4% yield).<sup>23</sup>  $R_f$  = 0.36 (DCM/methanol 10:1).  $^1\text{H}$  NMR (300 MHz, pyridine- $d_5$ ):  $\delta$  = 12.01 (s, 1H,  $\text{NHCO}$ ), 8.76 (d, 1H, 6-CH), 7.76 (d, 1H, 5-CH), 7.00 (t, 1H, 1'-CH), 5.14 (m, 1H, 3'-CH), 4.47–4.27 (overlapping m, 3H, 4'-CH and 5'- $\text{CH}_2$ ), 2.67 (t, 2H,  $\text{COCH}_2$ ), 1.79 (m, 2H,  $\text{COCH}_2\text{CH}_2$ ), 1.28 (m, 28H,  $(\text{CH}_2)_{14}$ ), 0.87 (t, 3H,  $\text{CH}_3$ ). ESI-HRMS  $[\text{M}+\text{H}]^+$   $m/z$  calculated for  $\text{C}_{27}\text{H}_{46}\text{F}_2\text{N}_3\text{O}_5$ : 530.3406, found: 530.3401.

**Acid-Sensitive Degradation. UV-vis spectroscopy.** PEG-C18 (i.e., PHC or PAC) was dissolved in phosphate buffered saline (PBS, 5 mM; pH 5.5, 6.8, or 7.4) to achieve the final concentration of 2 mg/mL and then incubated at 37  $^\circ\text{C}$  in a water bath. At predetermined time points, 0.2 mL of sample was withdrawn, and its absorbance at 500 nm was immediately measured using a BioTek Synergy HT Multi-Mode Microplate Reader (Winooski, VT). **High-resolution  $^1\text{H}$  NMR spectroscopy.** PEG-C18 in PBS (5 mM, pH 5.5, 6.8, or 7.4) at 2 mg/mL was incubated at 37  $^\circ\text{C}$  in a water bath. At predetermined time points, the pH value was adjusted to 8.0 using sodium hydroxide (NaOH, 0.25 or 0.5 N), and the samples were then lyophilized followed by high-resolution  $^1\text{H}$  NMR analysis using a Varian DirectDrive 600. The percentage of hydrolysis was calculated using the following equation:

$$\text{Percentage of hydrolysis (\%)} = \frac{S_{\delta 8.42}}{S_{\delta 8.42} + S_{\delta 9.82}} \times 100 \quad (1)$$

where  $S$  is the area of peak in  $^1\text{H}$  NMR spectrum and  $\delta$  is the chemical shift of the peak.

**Determination of the Critical Micellar Concentrations (CMC) of PEG-C18.** The CMC values of PHC and PAC in

water were determined using a pyrene 1:3 ratio method.<sup>28</sup> Briefly, 0.25 mL of pyrene in acetone (4.69  $\mu\text{g}/\text{mL}$ ) was added to a glass vial and dried under vacuum. Each vial was then supplemented with 2 mL of various concentrations (0.001–1 mg/mL) of PHC or PAC in aqueous solution. The glass vials were then capped and incubated overnight at room temperature while shaking at 200 rpm before further experiments. The samples were then subjected to fluorescence spectrometry (Fluorolog3 Fluorimeter, HORIBA Scientific, Edison, NJ). The emission spectra of pyrene were recorded between 350 to 450 nm (Ex = 335 nm, slit = 1 nm; Em slit = 2 nm). Five peaks were identified within this wavelength range and referred to as  $I_1$ ,  $I_2$ ,  $I_3$ ,  $I_4$ , and  $I_5$  from shorter to longer wavelengths. The intensity ratio between the first peak ( $I_1$ , 371 nm) and third peak ( $I_3$ , 383 nm) ( $I_1/I_3$ ) was calculated.

The values of CMC were obtained from the plot of the  $I_1/I_3$  ratio versus the logarithm of the concentration of PHC or PAC, which could be described by a decreasing sigmoid of the Boltzmann type using the following equation:<sup>28</sup>

$$y = \frac{A_1 - A_2}{1 + e^{(x-x_0)/\Delta x}} + A_2 \quad (2)$$

where the variable  $y$  corresponds to the  $I_1/I_3$  ratio, the independent variable  $x$  is the concentration of PHC or PAC,  $A_1$  and  $A_2$  are the upper and lower limits of the sigmoid, respectively,  $x_0$  is the center of the sigmoid, and  $\Delta x$  is directly related to the independent variable range where the abrupt change of the dependent variable occurs. For nonionic surfactants,  $x_0$  stands for the CMC value.

**Preparation and Characterization of GemC18-loaded PEG-C18 Micelles.** PEG-C18 micelles with different percentages of GemC18 (3%, 5%, or 10%,  $W_{\text{GemC18}}/W_{\text{PEG-C18}}$ ) were prepared using a modified thin-film hydration method. Briefly, 0.25 mL of THF containing 0.3, 0.5, or 1 mg of GemC18 was dried under vacuum and then hydrated with 1 mL of PAC or PHC aqueous solution (10 mg/mL) under vigorous stirring in a 75 °C water bath. Micelles were obtained within 5 min and then cooled down to room temperature with constant water bath sonication. The resultant micelle preparation was filtrated through a 0.2  $\mu\text{m}$  PTFE syringe filter (Nalge Nunc International, Rochester, NY), followed by lyophilization to obtain a white solid. Micelles with different percent of GemC18 were referred to as PHC3%, PHC5%, PHC10%, PAC3%, PAC5%, and PAC10%. To compare the intracellular fate of PHC and PAC micelles, a lipophilic fluorescence resonance energy transfer (FRET) pair, DiO and DiI were loaded into the micelles using the same method. DiI (0.25 mg) and DiO (0.25 mg) were added into each formulation (10 mg PHC or PAC) to achieve a theoretical loading of 5% ( $W_{\text{FRET pair}}/W_{\text{PEG-C18}}$ ). Finally, PHC and PAC micelles loaded with DiO (1%,  $W_{\text{DiO}}/W_{\text{PEG-C18}}$ ) only were also prepared to detect the intracellular localization of the micelles.

**Determination of Entrapment Efficiency and Percentage of Drug Loading.** To determine the concentration of GemC18, the lyophilized GemC18-loaded micelles were dissolved in THF and subjected to HPLC analysis using an Agilent 1260 Infinity Quaternary Liquid Chromatographic System with an UV detector operated at 248 nm and an Agilent ZORBAX Eclipse Plus C18 column (5  $\mu\text{m}$ , 4.6 mm  $\times$  150 mm). The mobile phase was methanol. The flow rate was 1 mL/min. The drug loading and the entrapment efficiency were calculated using the following equations:

$$\begin{aligned} \text{Percent of drug loading (\%)} \\ = \frac{\text{Weight of GemC18 in micelles}}{\text{Weight of GemC18 containing micelles}} \times 100 \end{aligned} \quad (3)$$

$$\begin{aligned} \text{Entrapment efficiency (\%)} \\ = \frac{\text{Weight of GemC18 in micelles}}{\text{Weight of total GemC18 added}} \times 100 \end{aligned} \quad (4)$$

**Determination of Particle Size and Zeta Potential.** The hydrodynamic diameters of blank micelles and GemC18-loaded micelles were determined using a Malvern Zetasizer Nano ZS (Malvern Instruments Ltd., MA). Lyophilized sample (1 mg) was dissolved in 1 mL of water and filtered through a 0.2  $\mu\text{m}$  PTFE filter prior to measurement. The zeta potential was determined using the same equipment, but lyophilized samples were dissolved in PBS (pH 7.4, 10 mM) at a final concentration of 1 mg/mL.

**Transmission Electron Micrographs (TEM).** The size and morphology of the micelles were examined using a Tecnai transmission electron microscope (FEI Company, Hillsboro, OR) in the Institute for Cellular and Molecular Biology Microscopy and Imaging Facility at The University of Texas at Austin. A carbon-coated 400-mesh copper specimen grid (Ted Pella, Inc., Redding, CA) was glow-discharged for 2 min. Micelle solutions (10 mg/mL) were deposited on the grid, and uranyl acetate staining were completed as described previously.<sup>29</sup>

**Drug Release from Micelles at Different pH.** GemC18-loaded micelles were dissolved in PBS (5 mM) with pH values of 5.5, 6.8, or 7.4 (50  $\mu\text{g}/\text{mL}$  GemC18) and incubated at 37 °C under constant shaking (150 rpm). At predetermined time points, 0.5 mL aliquots of sample were withdrawn, filtered through 0.2  $\mu\text{m}$  filter, and lyophilized. The lyophilized samples were dissolved in 0.5 mL of THF and centrifuged at 13 000 rpm for 10 min. The supernatants were subjected to HPLC analysis.

**In Vitro Stability in 10% FBS.** The stability of GemC18-loaded micelles was investigated by evaluating the changes in particle size and drug content after incubation in 10% FBS. Briefly, 450  $\mu\text{L}$  of GemC18-loaded micelles (1 mg/mL in water) were mixed with 50  $\mu\text{L}$  FBS. Particle sizes were recorded immediately and after 1 h of incubation at 37 °C. For drug content determination, the mixture was filtered (0.2  $\mu\text{m}$ ) after 1 h of incubation at 37 °C, and the filtrate was diluted with THF before applied to HPLC.

**In Vitro Cytotoxicity.** B16–F10 or BxPC-3 cells were seeded into 96-well plates (5000 cells/well). After overnight incubation, the culture medium was replaced with 200  $\mu\text{L}$  fresh medium containing GemHCl, GemC18 (less than 1.5% (v/v) dimethyl sulfoxide (DMSO) as a solubilizer), PHC5%, or PAC5%, with GemHCl-equivalent concentrations ranging from 0.7 to 7000 nM. After 48 h of incubation, the medium was replaced with 200  $\mu\text{L}$  of fresh culture medium containing 100  $\mu\text{g}$  of MTT. For BxPC-3 cells, formulations including GemHCl, PHC5%, PHC10%, PAC5%, and PAC10% were tested at GemHCl-equivalent concentrations of 14 and 140 nM. GemC18-free Blank PHC and PAC micelles were also tested at a concentration equivalent to 140 nM of GemHCl at 5% loading. Cells were incubated for four additional hours, followed by the addition of 200  $\mu\text{L}$  of DMSO to dissolve the purple formazan crystals formed after the removal of the MTT solution. The absorbance at 570 nm was measured using a

BioTek Synergy HT Multi-Mode Microplate Reader. Cell viability was calculated, and the IC<sub>50</sub> values were obtained using *Graphpad Prism* software (GraphPad Software, Inc., CA).

**Cellular Uptake and Metabolism.** B16–F10 cells ( $2.5 \times 10^5$ /well) were seeded in a 6-well plate and incubated overnight at 37 °C, 5% CO<sub>2</sub>. The medium was then replaced with 1 mL of fresh medium containing 20 μg/mL of GemC18, PHC5%, or PAC5% and incubated at 37 °C, 5% CO<sub>2</sub>. GemC18 solution was prepared by diluting GemC18 stock solution in DMSO with culture media (DMSO concentration at 1.35%, v/v). At predetermined time points (0.5, 1, 3, and 6 h), the culture medium was removed, cells were washed three times with cold PBS and then lysed with 1% SDS. The cell lysates were lyophilized and redissolved in methanol. The supernatant was collected after centrifugation and subjected to HPLC analysis to determine GemC18 concentration. To evaluate the cellular metabolism of GemC18, the GemC18-containing medium was removed after 6 h of incubation and replaced by fresh medium. After 16 additional hours of incubation, the amount of GemC18 in the medium and cells was determined using the same method as described above, which was divided by the amount of GemC18 initially taken up by the cells to obtain the percentage of GemC18 remaining.

**Intracellular Fate of PEG-C18 Micelles.** B16–F10 cells ( $5 \times 10^4$ /well) were seeded in a 35 mm glass-bottom dish (Mattek Corporation, Ashland, MA) and incubated overnight. To study the intracellular localization of PHC and PAC micelles, the cells were first treated with DiO-loaded PHC or PAC micelles (100 μg/mL in culture medium) (Ex/Em, 488/501 nm) for 3 h, followed by incubation with 500 nM Lyotracker Red DND-99 (an acidic organelle dye, Ex/Em, 577/590 nm) for 20 min and 5 μg/mL Hoechst 33342 (a nuclear dye, Ex/Em, 345/478 nm) for 5 min. Finally, the cells were rinsed with PBS and examined with a Leica TCS-SP5 confocal microscope with an oil immersion objective (63 × 1.4 NA) (Leica Microsystems GmbH, Mannheim, Germany).

For the purpose of comparing the intracellular fate of PHC and PAC micelles, the cells were first treated with 1.5 mL of medium containing 100 μg/mL of DiI/DiO-loaded PHC or PAC micelles for 3 h, followed by 0, 2, 6, or 24 h incubation after replacing the micelle-containing medium with fresh medium. Finally, the cells were examined using a Leica TCS-SP5 confocal microscope. Fluorescence images were acquired with the excitation wavelength of 488 nm, and the spectral filter of 555–655 nm (for DiI detection) was used to record FRET effect. All images were obtained with the same gain and offset. To further quantify the intracellular degradation of the micelles, cells pretreated with the DiI/DiO-loaded PHC or PAC micelles were incubated for 0, 2, 6, or 24 h with fresh medium, and then trypsinized and resuspended in PBS before being subjected to flow cytometry. Cell-associated fluorescence was analyzed using a Guava easyCyte 8HT Flow Cytometry System (Millipore Corporation, Billerica, MA) equipped with an argon laser (488 nm) and emission filter for 583 nm. Data collection involved 10 000 counts per sample. Data were analyzed using the *FlowJo* 9.3.1 software (Tree Star, Inc., Ashland, OR) and expressed as the geometric mean of the entire population. Cells incubated without micelles were used to account for background fluorescence.

**In Vivo Antitumor Activity.** All care and handling of animals were performed in accordance with National Institutes of Health guidelines, and the animal protocol was approved by the Institutional Animal Care and Use Committee at the

University of Texas at Austin. Female C57BL/6 mice (6–8 weeks) were from Charles River Laboratories (Wilmington, MA). The antitumor activity of the GemC18-loaded PEG-C18 micelles was evaluated in C57BL/6 mice with subcutaneously inoculated B16–F10 cells ( $5.0 \times 10^5$ /mouse) in the right flank. Treatments were given 6 days after tumor cell inoculation by tail vein injection with normal saline, GemHCl solution, GemC18 solution, blank PAC micelles, blank PHC micelles, PAC5% micelles, or PHC5% micelles. The dose was 0.283 mg of GemHCl or 0.283 mg of GemHCl-equivalent GemC18. GemC18 solution was prepared according to a previously reported method,<sup>21</sup> and all other formulations, including GemHCl and micelles, were dissolved in normal saline. All groups received a second dose three days after the first dose, while the PHC5% and PAC5% groups also received a third dose 3 days after the second dose. Tumor sizes were measured with calipers in two perpendicular diameters every day and reported as tumor volume ( $V = 1/2[a \times b^2]$ ,  $a$  = longest diameter,  $b$  = shortest diameter).

**Determination of Gemcitabine Concentration in Tumor Tissues and Plasma.** B16–F10 tumors were allowed to grow to ~1 cm<sup>3</sup> in C57BL/6 mice as mentioned above. GemHCl solution, GemC18 solution, PHC5%, or PAC5% was injected via the tail vein at a dose of 0.283 mg GemHCl-equivalent per mouse. Mice were sacrificed 4 h later, and the blood was collected into heparinized tubes and centrifuged (8000 rcf, 10 min) to isolate plasma. Tumor tissues were also collected, rinsed with cold saline, paper dried, and weighed before storing at –80 °C until analysis.

A hydrolysis method was used to detect the concentration of GemC18 in plasma.<sup>30</sup> Briefly, to 75 μL of plasma, 25 μL of AraU solution (10 μg/mL) was added as an internal standard, followed by the addition of 100 μL of 2 N NaOH. The mixture was vortexed and incubated at 40 °C for 1 h. After incubation, 0.8 mL of acetonitrile and 75 μL of 1.4 M H<sub>3</sub>PO<sub>4</sub> were added, followed by centrifugation at 13 000 rpm for 10 min. The supernatant was collected and dried under vacuum. The residue was redissolved in 100 μL of PBS (2.5 mM, pH 7.4) and centrifuged (13 000 rpm 10 min) again to collect the supernatant, which was then subjected to HPLC to measure gemcitabine concentration. The mobile phase was 5 mM sodium acetate (pH 6.0) and methanol (95/5, v/v), and the detection wavelength was 266 nm.

A direct extraction method was used to determine the concentration of GemC18 in tumor tissues. Briefly, around 100 mg of tumor tissue was homogenized in DCM using a bead beater (Biospec Products, Inc., Bartlesville, OK) at 4800 rpm for 80 s. Organic layers were collected after centrifugation (13 000 rpm, 10 min) and dried under vacuum. The residue was redissolved in 100 μL of methanol and centrifuged (13 000 rpm, 10 min) to collect the supernatant. The GemC18 concentration in the supernatant was determined using the same method as described above, while the detection wavelength of 308 nm was used.

**Histological Analyses.** For histological analyses, three representative tumors were harvested per experimental group at the end of treatment (day 6 for GemHCl solution, GemC18 solution, and normal saline groups; day 8 for PAC5% and PHC5% groups). Bromodeoxyuridine (BrdU) was injected intraperitoneally at a dose of 2 mg/mouse 30 min before euthanization. Tumor tissues were fixed with 10% buffered formalin phosphate, embedded in paraffin, sectioned (4 μm), stained with hematoxylin and eosin (H&E), and examined

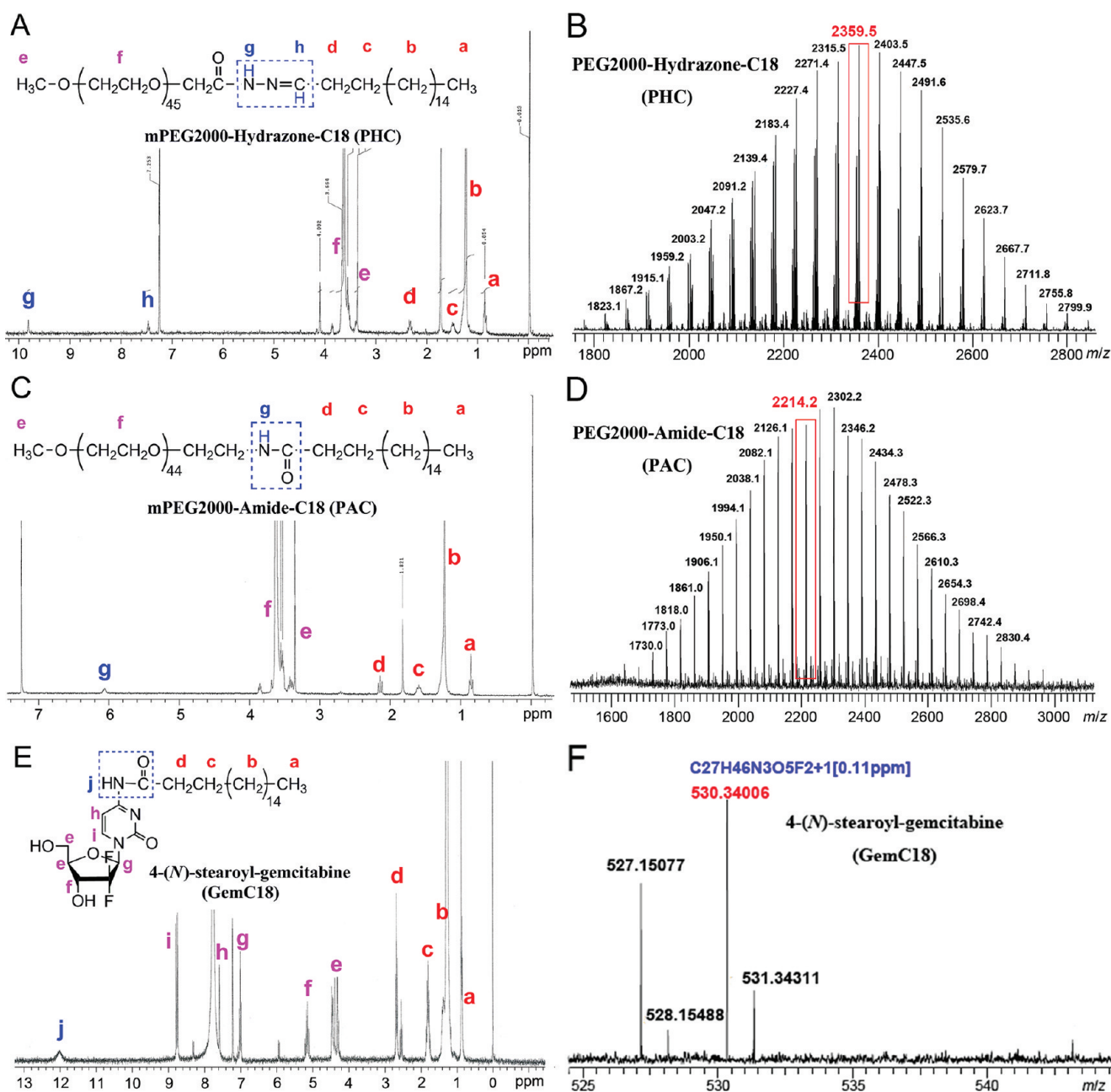


**Figure 1.** Characterization of PHC, PAC, and GemC18. (A)  $^1\text{H}$  NMR spectrum of PHC in  $\text{CDCl}_3$ . (B) MALDI mass spectrum of PHC. (C)  $^1\text{H}$  NMR spectrum of PAC in  $\text{CDCl}_3$ . (D) MALDI mass spectrum of PAC. (E)  $^1\text{H}$  NMR spectrum of GemC18 in pyridine- $d_5$ . (F) ESI-MS spectrum of GemC18.

under a light microscope. To detect the extent of tumor cell apoptosis, the slides were stained with TUNEL (Terminal deoxynucleotidyl Transferase Biotin-dUTP Nick End Labeling) and counterstained with 4',6-diamidino-2-phenylindole (DAPI) before visualized under an Olympus fluorescence microscope. The slides were also stained using anti-BrdU antibody at the University of Texas MD Anderson Cancer Center Science Park Research Division (Smithville, TX) to detect the extent of cell proliferation.

**Data Analysis.** All data are presented as mean  $\pm$  standard deviation (SD). Statistical analyses were completed by performing ANOVA followed by Fisher's protected least significant difference (LSD) procedure. A  $P$  value of  $\leq 0.05$  (two-tail) was considered significant.

## RESULTS

**Synthesis and Characterization of PHC, PAC, and GemC18.** PHC was synthesized by reacting PEG2000-hydrazide with octadecanal, which was first synthesized by oxidizing octadecanol. The appearance of aldehyde proton peak at 9.74 ppm in  $^1\text{H}$  NMR spectrum indicated the successful conversion of octadecanol to octadecanal (Figure S1 in Supporting Information). The most significant evidence of the formation of hydrazone bond after PEG2000-hydrazide was reacted with octadecanal includes (1) the chemical shift of the aldehyde proton from 9.74 ppm to 7.42 ppm (Figure 1A), which was due to the replacement of the aldehyde oxygen by the less electronegative nitrogen, and (2) the chemical shift of hydrazide proton ( $\text{CONHNH}_2$ ) from 8.42 ppm (Figure S2A)

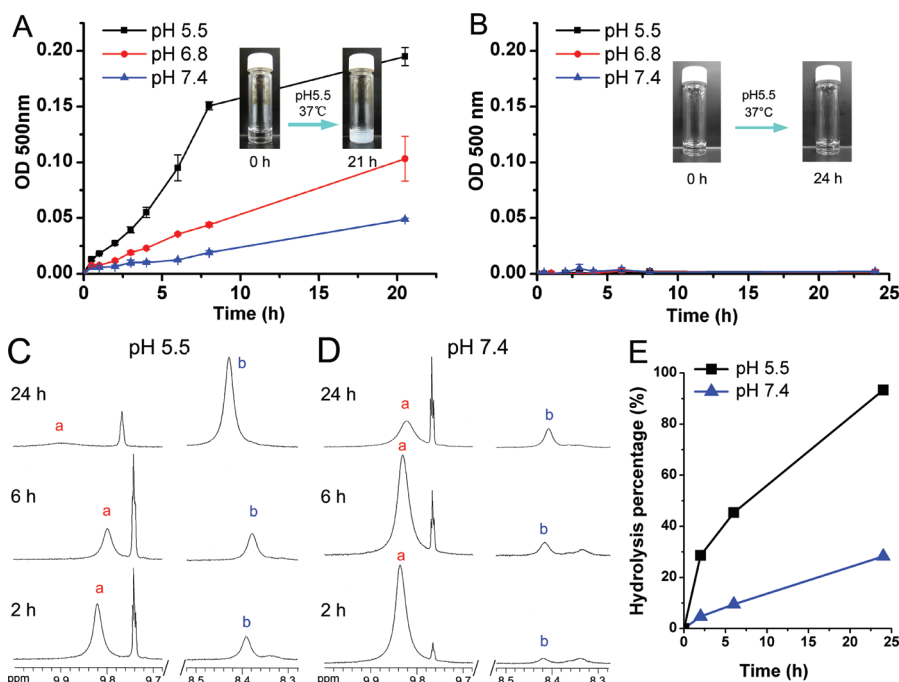


**Figure 2.** Acid sensitivity of PHC and PAC. (A) Time- and pH-dependent changes of the turbidity of PHC solution (insets are digital photographs taken after 0 and 21 h of incubation at pH 5.5, 37 °C). (B) Time- and pH-dependent changes of the turbidity of PAC solution. (C)  $^1\text{H}$  NMR spectra of PHC in  $\text{CDCl}_3$  after incubation for different periods of time at pH 5.5, 37 °C. (D)  $^1\text{H}$  NMR spectra of PHC in  $\text{CDCl}_3$  after incubation for different period of time at pH 7.4, 37 °C. (E) Time- and pH-dependent degradation of PHC based on  $^1\text{H}$  NMR spectra shown in C and D. a,  $\text{CONHN}=\text{CH}$  from PHC, 9.82 ppm; b,  $\text{CONHNH}_2$  from PEG2000-hydrazide, 8.42 ppm.

to 9.82 ppm ( $\text{CONHN}=\text{CH}$ ) (Figure 1A), which was due to the effect of  $\pi$ -bond from the newly formed carbon–nitrogen double bond. As will be shown later, these characteristic changes in chemical shift were also useful in quantifying the hydrolysis of PHC. The synthesis of PHC was further confirmed by matrix-assisted laser desorption/ionization (MALDI) mass spectrometry. The starting material of PEG2000-hydrazide has a molecular weight (MW) of 2087 ( $\text{H}^+$  adduct) (Figure S2B). After conjugation with octadecanal (MW 268, Figure S1B), a peak with  $m/z$  of 2359 ( $\text{Na}^+$  adduct) was observed in the MALDI mass spectrum of PHC (Figure 1B), which was in agreement with the expected MW of 2336.

PAC was synthesized by conjugating stearoyl chloride with PEG2000-amine. The  $^1\text{H}$  NMR spectrum of PAC is shown in Figure 1C, where the peak of 6.06 ppm ( $\text{NHCO}$ ) confirmed the formation of amide. For a comparison, the  $^1\text{H}$  NMR spectrum of PEG2000-amine could be found in Figure S3A. The MALDI mass data also supported the formation of PAC. The MW of PEG2000-amine was 1925 ( $\text{H}^+$  adduct) (Figure S3B), which was expected to increase to 2191 after conjugation with the stearoyl chloride (MW 303). The appearance of a peak with  $m/z$  of 2214 ( $\text{Na}^+$  adduct) confirmed the successful conjugation (Figure 1D).

GemC18 was synthesized by forming an amide bond between the aromatic amine of gemcitabine and stearic acid. Amide bond formation was confirmed by the appearance of a peak at 12.01 ppm in  $^1\text{H}$  NMR spectrum (Figure 1E). The electrospray ionization mass (ESI-MS) spectrum also provided evidence of the formation of GemC18 (Figure 1F).

**Acid Sensitivity of PEG-C18.** The acid sensitivity of the PEG-C18 (i.e., PHC or PAC) was first examined by UV–vis spectroscopy. The degradation of PHC and PAC was expected to produce water-insoluble octadecanal and stearic acid,

respectively, and result in an increase in the turbidity of the solution, providing a means to evaluate the degradation of the PEG-C18 by measuring the optical density of the solution at 500 nm ( $\text{OD}_{500\text{ nm}}$ ).<sup>31</sup> As shown in Figure 2A, PHC aqueous solution was transparent immediately after solubilization and did not have significant absorbance at 500 nm ( $\text{OD}_{500\text{ nm}}$  of 0). However, when incubated at pH 5.5, 37 °C, the PHC solution slowly became turbid, and the value of  $\text{OD}_{500\text{ nm}}$  increased to 0.195 after 21 h of incubation, which was likely due to the formation of water-insoluble octadecanal after the degradation of PHC. The increase of the  $\text{OD}_{500\text{ nm}}$  value for the PHC solution was slower at pH 6.8 than at pH 5.5; similarly, a slower increase in the  $\text{OD}_{500\text{ nm}}$  value was observed at pH 7.4 than at pH 6.8, indicating that the degradation of PHC was pH-dependent, faster at lower pH. In contrast, the turbidity of the PAC aqueous solution did not increase during 24 h of incubation at pH 5.5, 6.8, and 7.4, indicating that the PAC was stable at the pH tested (Figure 2B).

High-resolution  $^1\text{H}$  NMR spectroscopy (600 MHz) was used to further examine the pH-dependent degradation of PHC. As shown in Figure 2C, when PHC was incubated at pH 5.5, 37 °C, the peak area of the NH proton ( $\text{CONHN}=\text{CH}$ , 9.82 ppm) in the PHC molecule decreased as a function of time, while the peak area of the NH proton ( $\text{CONHNH}_2$ , 8.42 ppm) in the PEG2000-hydrazide increased gradually, indicating the disappearance of the PHC and the appearance of the PEG2000-hydrazide. A significant degradation was observed as early as after only 2 h of incubation, and almost all the PHC was degraded after 24 h of incubation (Figure 2C). A similar trend was observed at pH 7.4 (Figure 2D), but the degradation rate was much lower than at pH 5.5. Shown in Figure 2E are the changes of the peak area of characteristic protons as a function of time. Twenty-eight percent of PHC was hydrolyzed after

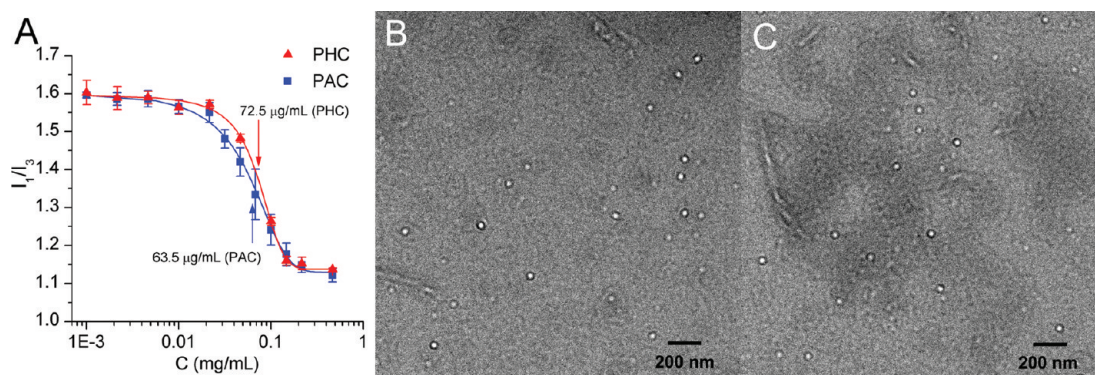


**Figure 3.** (A) Plots of  $I_1/I_3$  values versus the concentrations of PHC and PAC in water ( $n = 3$ ). (B) TEM image of PHC5% micelles. (C) TEM image of PAC5% micelles. Bar, 200 nm.

only 2 h of incubation at pH 5.5, and the percentage of hydrolysis increased to 45.4% and 93.3% after 6 and 24 h of incubation, respectively. In contrast, when incubated at pH 7.4, only 28.3% of PHC degraded after 24 h of incubation, again demonstrating the acid-sensitive degradation of the PHC. As to the PAC,  $^1\text{H}$  NMR data did not reveal any significant degradation after 24 h of incubation at pH 5.5 (data not shown).

**Preparation and Characterization of PEG-C18 Micelles.** The CMC value is an important characteristic of amphiphilic molecules, indicating the ability to form micelles. In the present study, the aggregation behavior of PEG-C18 was investigated by fluorescence spectroscopy using pyrene as a probe, which is sensitive to the polarity change of the microenvironment it is in. Figure 3A shows the fluorescence intensity ratio ( $I_1/I_3$ ) of pyrene as a function of the PEG-C18 concentration. At low PEG-C18 concentrations, pyrene mainly existed in the aqueous solution, and the  $I_1/I_3$  values remained constant ( $\sim 1.6$ ). As the concentration of PEG-C18 was increased, a substantial decrease in the  $I_1/I_3$  value was observed, indicating that pyrene was gradually transferred from the polar aqueous solution to the nonpolar core of the micelles.  $I_1/I_3$  values became constant ( $\sim 1.1$ ) again once all pyrene was completely incorporated into the micelles. After fitting the data into a decreasing sigmoid of the Boltzmann type, the CMC values of PHC and PAC were calculated to be  $72.5 \pm 0.3 \mu\text{g/mL}$  and  $63.5 \pm 14.2 \mu\text{g/mL}$ , respectively.

Formulation preparation was then performed by incorporating different amounts of GemC18 into PHC or PAC micelles. Micelles with different percentages of GemC18 (w/w) were referred to as PHC3%, PHC5%, PHC10%, PAC3%, PAC5%, and PAC10%. All micelles with or without GemC18 have similar slightly negative zeta potentials in PBS (10 mM, pH 7.4) (Table 1). Entrapment efficiency of more than 95% was obtained for all formulations (Table 1), and as expected, increasing the percentage of GemC18 included in the PHC or PAC micelles led to a decreased entrapment efficiency. Blank PHC and PAC micelles were  $21.6 \pm 0.6$  nm and  $12.8 \pm 0.1$  nm, respectively. The particle size increased after the incorporation of GemC18. For example, the size of PHC micelles increased to 29.6, 43.1, and 51.8 nm, respectively, when 3%, 5%, and 10% of GemC18 (w/w) was included (Table 1). Similar results were observed for the GemC18-loaded PAC micelles. The particle size was further confirmed by TEM. Both PHC5% micelles and PAC5% micelles exhibited uniform spherical shape, and the particle size determined from the TEM images was around 50

**Table 1. Characterization of PHC and PAC Micelles Loaded with or without GemC18 ( $n = 3$ )**

|         | entrapment efficiency (%) | drug loading (%) | particle size (nm) | zeta potential (mV) |
|---------|---------------------------|------------------|--------------------|---------------------|
| PHC     | -                         | -                | $21.6 \pm 0.6$     | $-3.3 \pm 1.1$      |
| PHC 3%  | $99.5 \pm 3.0$            | $3.3 \pm 0.1$    | $29.6 \pm 3.7$     | $-2.7 \pm 1.2$      |
| PHC 5%  | $96.7 \pm 2.5$            | $5.0 \pm 0.1$    | $43.1 \pm 3.8$     | $-2.0 \pm 0.7$      |
| PHC 10% | $95.9 \pm 6.5$            | $9.7 \pm 1.3$    | $51.8 \pm 3.2$     | $-2.2 \pm 0.9$      |
| PAC     | -                         | -                | $12.8 \pm 0.1$     | $-1.6 \pm 0.5$      |
| PAC 3%  | $102.1 \pm 2.5$           | $3.5 \pm 0.3$    | $28.1 \pm 1.0$     | $-1.8 \pm 0.6$      |
| PAC 5%  | $101.1 \pm 7.7$           | $5.5 \pm 0.4$    | $40.8 \pm 2.8$     | $-1.6 \pm 0.4$      |
| PAC 10% | $95.6 \pm 11.3$           | $9.7 \pm 0.5$    | $45.3 \pm 2.7$     | $-1.7 \pm 0.5$      |

nm (Figure 3B,C), in agreement with that measured by the dynamic laser scattering technique (Table 1).

**In Vitro Stability of GemC18-Loaded Micelles.** The GemC18-loaded micelles are intended to be administrated intravenously. Therefore, the physical and chemical stabilities of them in 10% FBS were evaluated to estimate the extent to which they would aggregate upon i.v. injection. As seen in Figure 4A, the size of the GemC18-loaded micelles did not change after 1 h of incubation in 10% FBS ( $P > 0.05$ ). It should be noted that, due to the small size ( $\sim 10$  nm) of the proteins in the FBS, the overall average particle size of GemC18-loaded micelles measured using the dynamic light scattering technique decreased slightly after mixing with FBS. Figure 4B showed the percentage of GemC18 remaining in micelles after 1 h of incubation with FBS at 37 °C; more than 94% of the GemC18 remained in the micelles after 1 h of incubation with FBS at 37 °C when the drug loading percentage was at 3% and 5%. However, for PHC10% and PAC10%, the percentage of GemC18 remaining decreased to about 86% after the same period of incubation. According to the stability data in Figure 4, the PHC5% and PAC5% were chosen for further *in vitro* and *in vivo* studies, considering the relatively high concentration of GemC18 in them and their relatively higher stability.

**In Vitro Release of GemC18 from PHC5% and PAC5%.** Acid-sensitive release of GemC18 from PHC5% and PAC5% was investigated at different pH. As seen in Figure 5A, the rate of release of GemC18 from PHC5% was pH-dependent. At pH 5.5,  $93.1 \pm 7.2\%$  of the GemC18 was still in the micelles after 2 h of incubation, but almost all the GemC18 was released after another 2 h of incubation. At pH 6.8, PHC5% remained stable for at least 8 h, and a complete release was observed only after 24 h of incubation. At pH 7.4, about 80% of the GemC18 still

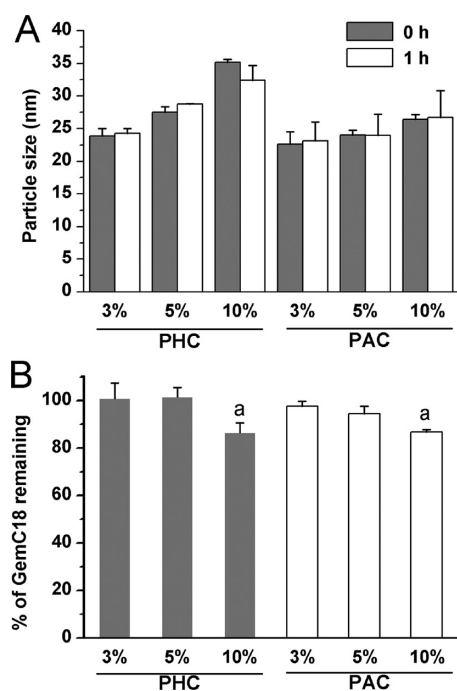


**Figure 4.** *In vitro* stability of GemC18-loaded PHC and PAC micelles. (A) Particle sizes of PHC and PAC micelles loaded with various percentages of GemC18 after 1 h of incubation with 10% FBS at 37 °C. (B) The percentage of GemC18 remaining in PHC and PAC micelles after 1 h of incubation with 10% FBS at 37 °C ( $n = 3$ ). a,  $P < 0.05$  vs 3% and 5%.

remained in the micelles even after 24 h of incubation. In contrast, no apparent pH-dependent GemC18 release was observed from the PAC5% micelles (Figure 5B). Close to 90%

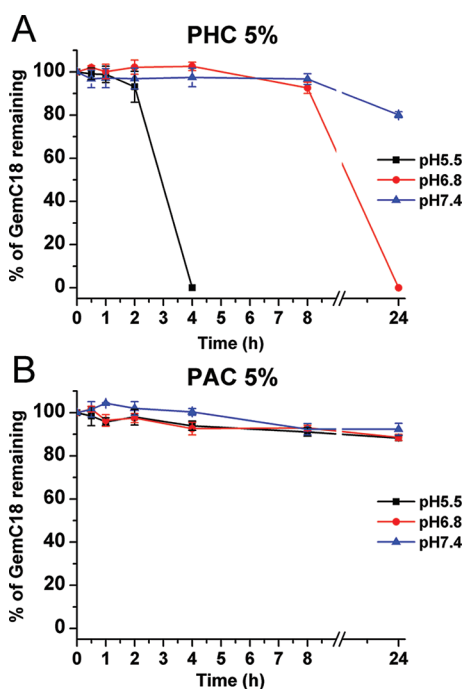


**Figure 5.** Release of GemC18 from PHC5% (A) and PAC5% (B) micelles in PBS of different pH values (5.5, 6.8, and 7.4) at 37 °C ( $n = 3$ ).

of the GemC18 still remained in the micelles after 24 h of incubation at all pH values.

**In Vitro Cytotoxicity.** The cytotoxicity of the GemC18 in PHC or PAC micelles was evaluated by determining the viability of cells after incubation with the micelles using the MTT assay. The BxPC-3 human pancreatic cancer cell line was used first in a preliminary study. It was reported that the  $IC_{50}$  value of GemHCl was around 14 nM in BxPC-3 cells.<sup>23</sup> Therefore, we tested the cytotoxicity of the GemC18 in micelles at 14 and 140 nM. As shown in Figure 6A, the PHC

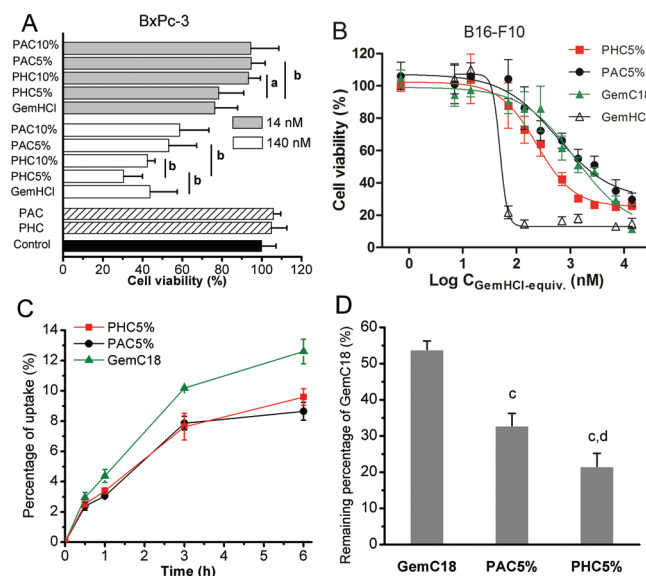


**Figure 6.** (A) Viability of BxPC-3 cells after 48 h of incubation with 14 nM or 140 nM of GemHCl or GemC18 in micelles ( $n = 5$ ). a,  $P < 0.05$ ; b,  $P < 0.01$ . The concentrations of blank PHC and PAC micelles were equivalent to 140 nM of GemC18 at 5% loading. (B) Viability of B16-F10 cells after 48 h of incubation with GemHCl, GemC18, PHC5%, or PAC5% micelles ( $n = 4$ ). (C) Percentage of GemC18 internalized by B16-F10 cells after incubation with GemC18 in solution or in PHC5% or PAC5% micelles ( $n = 3$ ). (D) Percentage of GemC18 remaining in B16-F10 cells 16 h after internalization ( $n = 3$ ). c,  $P < 0.01$  vs GemC18; d,  $P < 0.01$  vs PAC5%.

micelles were more cytotoxic than PAC micelles, and for the PHC micelles, micelles with 5% of GemC18 were more cytotoxic than those with 10% GemC18 ( $P < 0.05$  and  $P < 0.01$  at 14 nM and 140 nM, respectively). In addition, it was also found that the cytotoxicity of PHC5% was comparable to that of the GemHCl at 14 nM, and was even higher at 140 nM ( $P < 0.01$ ). Finally, we have also tested the cytotoxicity of the blank micelles. As seen in Figure 6A, blank PHC and PAC micelles, at a concentration equivalent to 140 nM of GemC18 at 5% loading, did not show any significant cytotoxicity, confirming that the cytotoxicity of GemC18 in micelles was not due to the PHC or PAC molecules themselves. The cytotoxicity data were also supportive of using 5% drug loading in the future work.

Figure 6B showed the viability of B16-F10 cells after 48 h of incubation with GemHCl, GemC18, PHC5%, or PAC5%. GemHCl had the strongest cytotoxicity with an  $IC_{50}$  value of 48.9 nM. The prodrug GemC18 was significantly less cytotoxic than GemHCl, with an  $IC_{50}$  value almost 20 times higher (1227 nM). However, incorporation of the GemC18 into PHC or PAC micelles significantly decreased the  $IC_{50}$  values to 233.7 nM and 556.7 nM, respectively, indicating an increase in the cytotoxicity of the GemC18 after incorporation into micelles.

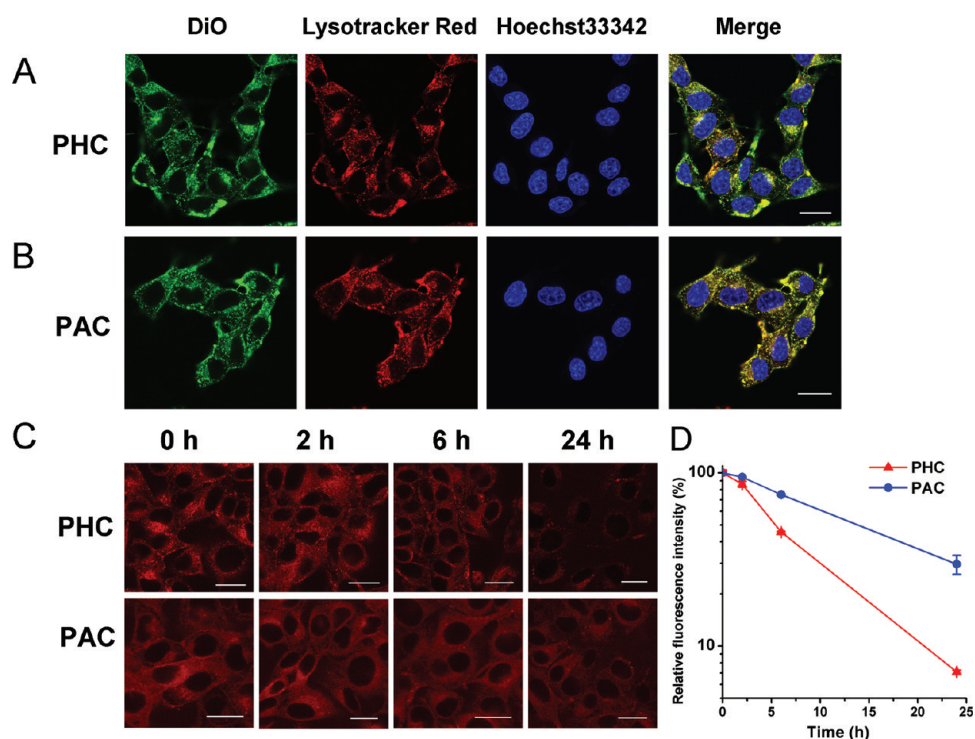


**Figure 7.** Comparison of intracellular fate of PHC and PAC micelles. (A) Colocalization of DiO-loaded PHC micelles (green) with lysosomes (red). Cell nuclei are in blue. (B) Colocalization of DiO-loaded PAC micelles with lysosomes. (C) Time-dependent decrease of FRET effect in B16–F10 cells preincubated with DiI/DiO-loaded PHC micelles or PAC micelles. (D) Time-dependent decrease of FRET effect quantified by flow cytometry ( $n = 3$ ).

Finally, PHC5% was more cytotoxic than PAC5% against B16–F10 cells (Figure 6B).

**Cellular Uptake of GemC18 in Micelles and Its Intracellular Metabolism.** The cellular uptake of GemC18 in solution and in micelles was studied by directly determining the concentration of GemC18 in cells using an HPLC method. As seen in Figure 6C, the uptake of GemC18 was time-dependent. GemC18 dissolved in culture medium (with 1.35% DMSO, v/v) was more efficiently taken up by B16–F10 cells than GemC18 in micelles, with  $12.6 \pm 0.8\%$  of GemC18 in solution being internalized after 6 h of incubation, while the percentage of GemC18 in PHC5% and PAC5% that was internalized was  $9.6 \pm 0.5\%$  and  $8.7 \pm 0.6\%$ , respectively.

Figure 6D showed the intracellular stability of the internalized GemC18. When the GemC18 was internalized as GemC18 in solution,  $53.9 \pm 2.4\%$  of it was recovered after 16 h in cells. However, only  $32.8 \pm 3.4\%$  and  $21.6 \pm 3.7\%$  of GemC18 remained in the cells 16 h after it was internalized as PAC5% or PHC5%, respectively, indicating a higher degree of cellular metabolism of GemC18 when it was taken up by the cells as GemC18-loaded micelles, especially in the acid-sensitive PHC micelles.

**Intracellular Localization and Acid Sensitivity of GemC18 in Micelles.** Localization of acid-sensitive micelles in acidic organelles after cellular uptake is a prerequisite for acid-sensitive drug release. In the present study, DiO-loaded PHC or PAC micelles were used to identify the intracellular localization of the micelles. As seen in Figure 7A, almost all the PHC micelles were located in the lysosomes, showing an almost complete overlap with LysoTracker red, which was a marker specific to late endosomes and lysosomes. A similar overlap was observed with the PAC micelles (Figure 7B),

indicating the efficient accumulation of both micelles into the acidic organelles after cellular uptake.

FRET is a physical property of energy transfer from a donor dye to an acceptor dye. If both dyes existed within the range of Förster distance, nonradiative fluorescence from the excited donor dye could be effectively used as the excitation energy for the acceptor dye, resulting in the emission of the acceptor fluorescence.<sup>32</sup> Therefore, for micelles with both DiO (donor, Ex/Em 488/501 nm) and DiI (acceptor, Ex/Em 501/565 nm) inside, when they are excited at wavelength of 488 nm, the energy generated from DiO can be transferred to DiI, which subsequently emits a red fluorescence. With the degradation of micelles and/or the release of DiO/DiI from them, the FRET effect is expected to decrease, accompanied by the decrease of red fluorescence. As seen in Figure 7C, cells preincubated with the DiO/DiI-loaded PHC and PAC micelles gave bright red color when observed under a confocal microscope. For the PHC micelles, a significant decrease in fluorescence intensity was observed 6 h later, and almost all the fluorescence disappeared 24 h later. However, cells preincubated with the PAC micelles kept almost the same fluorescence intensity 6 h later, and a significant decrease in fluorescence intensity was observed only 24 h later. Moreover, flow cytometric data also confirmed the observation from the confocal microscope. As seen in Figure 7D, the mean fluorescence intensity of cells preincubated with DiI/DiO-loaded PHC micelles decreased significantly faster than that of cells preincubated with the PAC micelles.

**In Vivo Antitumor Activity.** To evaluate the *in vivo* antitumor activity of the GemC18 in micelles, B16–F10-tumor-bearing mice were treated with normal saline, GemHCl solution, GemC18 solution, blank PAC, blank PHC, PAC5% micelles, or PHC5% micelles. As seen in Figure 8A, tumors in

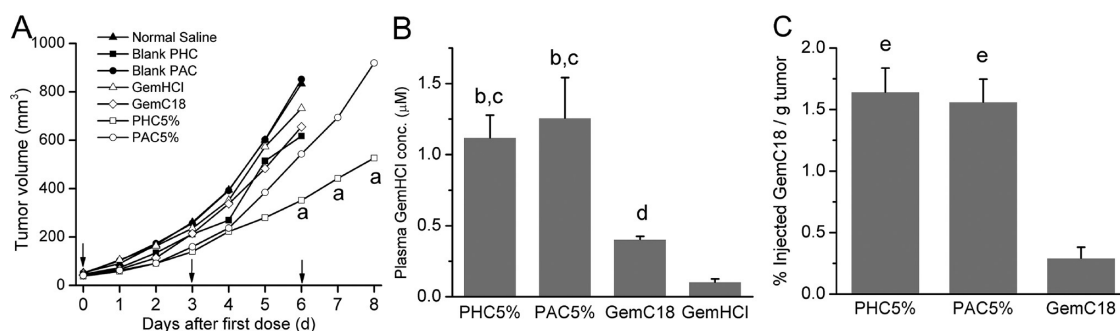


**Figure 8.** (A) Effect of normal saline, GemHCl in solution, GemC18 in solution, blank PHC micelles, blank PAC micelles, PHC5%, or PAC5% on the growth of murine B16–F10 tumors in C57BL/6 mice ( $n = 5–8$ ). Arrows indicated the days of injection. a,  $P < 0.05$  vs PAC5%. (B) Plasma concentration of gemcitabine after i.v. injection of GemHCl in solution, GemC18 in solution, PHC5%, or PAC5% (expressed as GemHCl-equiv,  $n = 4$ ). b, c,  $P < 0.01$  vs GemC18 and GemHCl, respectively; d,  $P < 0.01$  vs GemHCl. (C) Percentage of GemC18 accumulated into tumor tissues 4 h after i.v. injection of GemC18 in solution, PHC5%, or PAC5% at a dose of 0.5 mg GemC18 per mouse ( $n = 4$ ). e,  $P < 0.01$  vs GemC18.

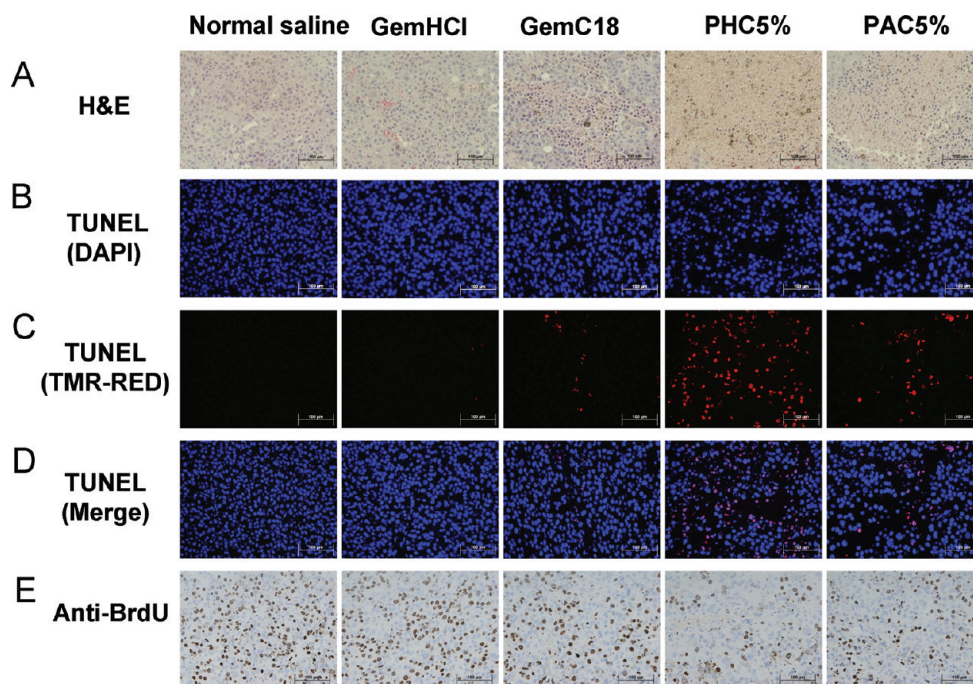


**Figure 9.** (Immuno)histograms of murine B16–F10 tumors after mice were treated with normal saline, GemHCl in solution, GemC18 in solution, PHC5%, or PAC5%. (A) H&E staining. (B–D) TUNEL staining. (E) Anti-BrdU staining.

mice that were injected with normal saline grew aggressively and uncontrolled, and the tumor volume reached  $833 \pm 274$  mm<sup>3</sup> six days after the first injection. No significant difference in tumor volume was observed between mice that were injected with the blank micelles and normal saline, indicating that the blank micelles were pharmaceutically inert, and any therapeutic effect from the PAC5% and PHC5% micelles should be attributed to the GemC18 in the micelles. The sizes of the tumors in mice that were injected with GemHCl or GemC18 in solution were not significantly different from that in mice that were injected with normal saline at the end of treatment (day 6,  $P = 0.50$  and  $0.19$  compared to GemHCl and GemC18, respectively). In contrast, PAC5% and PHC5% significantly inhibited the tumor growth compared with normal saline, which was significant as early as on the second day after the first dose ( $P < 0.05$ ). On the first 5 days after the first dose, PHC5% and PAC5% were equally effective in inhibiting tumor growth (day 5,  $P = 0.11$ ). Starting on day 6, the mean size of tumors in mice that were treated with the PHC5% micelles became

significantly smaller than that in mice that were treated with the PAC5% micelles. Finally, the body weights of mice that received various treatments were also recorded. A slight increase in body weight was observed at the end of treatment, but no significant difference was observed among the different groups of mice (data not shown).

**Plasma Concentration and Tumor Accumulation of Gemcitabine or GemC18.** After i.v. injection, GemHCl was quickly cleared from the circulation, with a plasma GemHCl concentration of only  $0.11 \pm 0.02$  μM 4 h after i.v. injection (Figure 8B). The clearance of GemC18 was slightly slower with a plasma GemC18 concentration of  $0.40 \pm 0.02$  μM 4 h after i.v. injection of GemC18 in solution. When GemC18 was incorporated into micelles, its clearance was further slowed down. For example, the plasma GemC18 concentration was  $1.12 \pm 0.16$  μM and  $1.26 \pm 0.28$  μM for the PHC5% and PAC5% micelles, respectively, 4 h after i.v. injection.

The PHC and PAC micelles also increased the accumulation of GemC18 in tumors. As shown in Figure 8C, 4 h after i.v.

injection, the concentrations of GemC18 in tumors reached  $1.64 \pm 0.19\%$  and  $1.56 \pm 0.18\%$  of the injected amount (per g of tumor), when mice were injected with PHC5% and PAC5%, respectively, which are more than 5 times higher than when mice were injected with GemC18 in solution.

**Histology.** Hematoxylin and eosin (H&E) staining revealed that tumors in mice that were treated with normal saline were characteristic of large nuclei, with small intercellular spaces (Figure 9A). Tumors in mice that were treated with GemHCl or GemC18 displayed similar characteristics, indicating a limited therapeutic effect. However, treatment with PHC5% or PAC5% micelles led to a significant shrinkage of the nuclei and much larger intercellular spaces, with the PHC5% being stronger than PAC5% (Figure 9A). Apoptotic cells (purple) were detected only in tumors in mice that were treated with GemC18 in PHC or PAC micelles, and the GemC18 in PHC micelles (PHC5%) appeared to induce more apoptosis in tumor tissues than the GemC18 in PAC micelles (PAC5%) (Figure 9B–D). Antibromodeoxyuridine (BrdU) staining showed extensive cell proliferation in tumors in mice that were injected with normal saline. Treatment with GemHCl or GemC18 solution did not significantly decrease the extent of cell proliferation. However, a significant decrease in BrdU positive staining was observed in tumors in mice that were treated with PHC5% or PAC5% micelles, as compared with that in mice that were treated with normal saline, and it appeared that the BrdU positive staining was significantly less extensive in tumors in mice that were treated with the PHC5% micelles than with the PAC5% micelles (Figure 9E).

## DISCUSSION

In the present study, we reported a new method to construct acid-sensitive micelles by directly conjugating hydrophilic PEG with a hydrophobic stearic acid derivative (C18) using an acid-sensitive hydrazone bond. The acid sensitivity of the PHC micelles was validated both in test tube and in cells in culture. Specifically, to the best of our knowledge, this represents the first report using FRET technique to confirm the cellular-level acid sensitivity of acid-sensitive micelles. The PHC micelles as a carrier to a lipophilic prodrug, 4-(*N*)-stearoyl gemcitabine (GemC18), significantly enhanced the *in vitro* and *in vivo* antitumor activity. The enhanced antitumor activity may be attributed to the enhanced plasma retention and tumor accumulation of GemC18 by the micelles, the lysosomal delivery of GemC18, and faster acid-sensitive release of GemC18 from the PHC micelles in lysosomes.

The lack of stability after systemic injection is a major obstacle preventing the development of effective micelle drug delivery systems, which could be reflected as follows:<sup>33</sup> (1) micelle dissociation upon dilution in the blood, (2) particle size increase due to micelle aggregation or protein binding, (3) and drug loss caused by plasma protein extraction or protein-induced micelle disassembly. The effect of blood dilution could be alleviated by using amphiphilic molecules with a low CMC value. Because of the lower molecular weight of the hydrophobic C18 group, the CMC values of the PEG-C18 synthesized in the present study ( $\sim 70 \mu\text{g/mL}$ ) were relatively higher than that of previously reported synthetic block copolymers ( $\sim 4 \mu\text{g/mL}$ ),<sup>34,35</sup> yet they were still much lower than that of commonly used nonionic surfactants, such as Tween 80 and Tween 20 (both  $\sim 300 \mu\text{g/mL}$ ),<sup>36</sup> and comparable with that of Pluronic block copolymers (25, 35, and  $299 \mu\text{g/mL}$  for Pluronic P123, F127, and P85,

respectively).<sup>37</sup> On the basis of the blood volume of a mouse ( $58.5 \text{ mL}$  of blood per kg of body weight)<sup>38</sup> and the dose of the micelles injected ( $9.5 \text{ mg}$  of PEG-C18), we estimated that the concentration of PEG-C18 in the blood of a mouse of  $25 \text{ g}$  can be as high as  $6.75 \text{ mg/mL}$ , which was about 100 times higher than the CMC values of PEG-18 ( $60\text{--}70 \mu\text{g/mL}$ ). Therefore, it is expected that micelles formed by PEG-C18 are potentially stable against dilution when used as drug carriers. The effect of serum/plasma proteins on the stability of the micelles formed was also evaluated by measuring the particle size changes and the loss of GemC18 from the micelles after incubation with 10% FBS. The fact that no significant change in particle size was observed and that more than 94% of the GemC18 still remained in the micelles (at lower loading percentages of 3–5%) after 1 h of incubation with 10% FBS suggested that the GemC18-loaded micelles were resistant to protein-induced aggregation and extraction (Figure 4).

The results from the release study also demonstrated the stability of the GemC18-loaded micelles. For acid-insensitive PAC micelles, only 10% of GemC18 was released after 24 h of incubation (Figure 5B); for acid-sensitive PHC micelles, the percent of GemC18 released after 24 h of incubation at pH 7.4 was around 20% (Figure 5A), indicating that the GemC18-loaded PEG-C18 micelles were able to retain the incorporated GemC18. Rijcken et al. stated that the slow release of drugs from micelles could be attributed to the solid-like core of the polymeric micelles and the high affinity between drug molecules and the hydrophobic core of micelles.<sup>10</sup> It is unlikely that the PEG-C18 micelles had a solid-like core, since similar micelles prepared with 1,2-distearoyl-*sn*-glycero-3-phosphoethanolamine (DSPE)-PEG2000 were reported to have a fluid core.<sup>39</sup> A possible explanation for the slow release of GemC18 from the PEG-C18 micelles may be attributed to the high affinity between the C18 chains of GemC18 and the PEG-C18. It is well-recognized that fatty acid chains stabilize and hold together the phospholipid bilayers of the cell membrane by a variety of forces such as van der Waals interactions.<sup>40</sup>

Being stable in the blood circulation after i.v. injection is beneficial to the therapeutic effect of micelle drug delivery systems against tumors. However, for acid-sensitive micelles, it is also critical for them to readily release drug in an acidic condition. Polymeric micelles with a semisolid core suffer from the risk of core precipitation after the removal of the hydrophilic segment, which may explain why there is no report of constructing acid-sensitive micelles by directly conjugating a hydrophobic polymer with a hydrophilic polymer using an acid-sensitive bond. It is unlikely that the current PEG-C18 micelles have a hydrophobic core as “solid” as that of a polymeric micelle. Therefore, core precipitation was unlikely after the cleavage of the hydrazone bond. This was confirmed by the confocal microscopy data using DiI/DiO-loaded PEG-C18 micelles. The almost complete disappearance of FRET effect (i.e., the red fluorescence in Figure 7C) indicated the release of DiI and DiO from the micelle core. Otherwise, the FRET effect should not have disappeared if core precipitation happened. Therefore, the GemC18-loaded PEG-C18 micelles are expected to be stable at neutral pH in the blood circulation, but able to readily release GemC18 in an acidic condition.

In fact, the acid sensitivity of the PHC molecule and GemC18-loaded PHC micelles was demonstrated both in test tubes and in cells in culture. The acid sensitivity of the PHC was first examined by UV-vis spectroscopy and high-resolution <sup>1</sup>H NMR spectroscopy. PHC was found to be acid-sensitive,

while the control PAC was stable at pH 5.5, 6.8, and 7.4 (Figure 2B). The degradation data of PHC (Figure 2E) showed that 29–40% of PHC was hydrolyzed after 2–4 h of incubation at pH 5.5. Meanwhile, within 2–4 h of incubation at the same pH, the percentage of GemC18 released from the PHC micelles sharply increased from 7% to 100% (Figure 5). Similarly, at pH 7.4, the release of GemC18 from the micelles was negligible at 6 h when only 9.5% of PHC was degraded, while 28.3% of PHC degradation led to 20% of release of GemC18. Taken together, it appears that, when 30–40% of the PHC was hydrolyzed, the PHC micelles underwent dissociation, resulting in the complete release of GemC18.

The cellular-level acid sensitivity of acid-sensitive micelles had rarely been investigated previously. Previously, FRET technique was used to study the stability of PEG-poly(lactic acid) (PLA) micelles after i.v. administration<sup>41</sup> or after incubation with cells.<sup>42</sup> Xiao et al. also used FRET technique to evaluate the interaction between PEG-PLA micelles and the cell membrane.<sup>43</sup> In the present study, we evaluated the acid sensitivity of the PEG-C18 micelles at the cellular level using FRET. Using the intensity of red fluorescence generated from the FRET effect as the indicator, both confocal microscopic images and the flow cytometric data revealed that the FRET effect diminished faster in cells preincubated with the PHC micelles than in cells preincubated with the PAC micelles (Figure 7C,D), which was likely caused by the acidic lysosomal condition, confirming the cellular-level acid sensitivity of PHC micelles. This finding is in agreement with the lysosomal delivery of the PEG-C18 micelles (Figure 7A,B) and the different release profiles of the GemC18 from the micelles in acidic conditions in tubes (Figure 5). Finally, although to a lesser degree, a decrease in red fluorescence was also observed when cells were preincubated with the PAC micelles, indicating that the micelles also underwent destabilization inside cells independent of the acidic condition.

Acid-sensitive destabilization of micelles either extracellularly or intracellularly followed by the quick release of anticancer drugs incorporated in them should be beneficial to the antitumor activity of the anticancer drug. However, GemC18 is a prodrug, which needs to be hydrolyzed to produce the active gemcitabine. The amide bond is relatively stable in physiological and slightly acidic conditions,<sup>44</sup> but its hydrolysis is enzymatically catalyzed by enzymes such as cathepsin B (a cysteine protease) and cathepsin D (an aspartic protease),<sup>21</sup> which are important enzymes in lysosomes and play a key role in the degradation of amide-bearing drugs, polypeptides, and proteins inside cells.<sup>45</sup> Therefore, it is preferable to specifically deliver the GemC18 into the lysosomes. The *in vitro* cellular uptake and cytotoxicity data are also supportive of the delivery of the GemC18 into lysosomes by the micelles. Even though the cellular uptake of the GemC18 in solution was 30–40% higher than the uptake of the GemC18 in PHC or PAC micelles (Figure 6C), the cytotoxicity of the GemC18 in solution was lower (Figure 6B), likely because the GemC18 in solution entered the cells by passive diffusion and was distributed randomly over the whole cell. In contrast, the micelles entered cells by endocytosis, were transferred into the lysosomes, and then released the GemC18 by acid-sensitive micelle destabilization. The GemC18 released into the lysosomes was then enzymatically hydrolyzed to generate gemcitabine. The faster disappearance of GemC18 in cells when delivered using the micelles than using GemC18 in solution and, more importantly, the faster disappearance of the

GemC18 in cells when delivered using the acid-sensitive PHC micelles than using the acid-insensitive PAC micelles (Figure 6D) are supportive of the reasoning above. The newly generated gemcitabine may cross the lysosome membrane and reach the cytoplasm by passive diffusion<sup>46</sup> and/or with the help of human equilibrative nucleoside transporter 3 (hENT3), which is localized in the late endosomes/lysosomes.<sup>47</sup>

Finally, the *in vivo* antitumor activity of GemC18 in the acid-sensitive PHC micelles was evaluated in C57BL/6 mice with the model of B16–F10 melanoma. The B16–F10 mouse melanoma model was chosen because the B16–F10 tumor cells grew aggressively in the syngeneic C57BL/6 mice, which allowed us to readily determine whether the delivery of the GemC18 in the acid-sensitive PHC micelles can improve its *in vivo* antitumor activity. After all, melanoma is the most dangerous skin cancer, causing the majority of deaths related to skin cancer, and clinical data showed that melanoma is responsive to gemcitabine.<sup>18,19</sup> GemHCl or GemC18 in solution did not show any significant antitumor activity (Figure 8A). It is possible that a higher dose of GemHCl or GemC18 in solution is needed for them to show antitumor activity against the B16–F10 tumor in mice. In addition, both GemHCl and GemC18 are small molecules and could be quickly eliminated after i.v. injection. They may have also distributed to organs and tissues other than tumors. Data in Figure 8A showed that the GemC18 in micelles was more effective than GemC18 in solution and GemHCl in solution in inhibiting the tumor growth, which may be attributed to the following: (1) The hydrophilic PEG corona on the micelles created a barrier layer to block the adhesion of opsonins present in the serum, thus preventing the recognition of the micelles by phagocytic cells, reducing the accumulation them in the reticuloendothelial system (RES), and prolonging their circulation in blood.<sup>9</sup> (2) The nanoscaled size (40–50 nm) of the micelles permitted the passive accumulation of them in tumor tissues due to the EPR effect.<sup>33</sup> (3) The micelles delivered GemC18 into the lysosomes, where enzymatic hydrolysis facilitated the generation of the active parent drug of gemcitabine after GemC18 release. More importantly, we have found that the acid-sensitive PHC5% micelles were more effective than the acid-insensitive PAC5% micelles in inhibiting the tumor growth (Figure 8A). Possible explanations are summarized as follows: (1) intravenous injection of either PHC5% or PAC5% resulted in comparable plasma GemC18 concentrations and accumulations of GemC18 in the tumor tissues (Figure 8B,C); (2) the cellular uptakes of PHC5% and PAC5% were also similar (Figure 6C); (3) the GemC18 was more quickly released from acid-sensitive PHC5% micelles than from the acid-insensitive PAC5% micelles, which was confirmed both in test tube in acidic condition (Figure 5) and in cultured cells (Figure 7); (4) due to the faster release of GemC18 from the PHC micelles than from the PAC micelles, the GemC18 delivered using the PHC micelles can be more quickly hydrolyzed to regenerate gemcitabine, which was supported by Figure 6D. The histological data, including H&E, TUNEL, and anti-BrdU staining, also confirmed that the acid-sensitive PHC5% micelles induced more tumor cell apoptosis and more effectively inhibited tumor cell proliferation than the acid-insensitive PAC5% micelles, supporting the finding that the PHC5% micelles were more effective than the PAC5% micelles in inhibiting tumor growth (Figure 8A).

## CONCLUSION

In the present study, we reported a novel strategy to construct acid-sensitive micelles by directly conjugating the hydrophilic PEG with a hydrophobic stearic acid derivative (C18) using an acid-sensitive hydrazone bond. Furthermore, the anticancer drug gemcitabine was conjugated with stearic acid (C18) to produce the lipophilic prodrug, namely, GemC18, which was then incorporated into the micelles. Acid-sensitive release was observed when the micelles were incubated in slightly acidic conditions, while the control PAC micelles were stable at the same incubation conditions. Cellular-level acid sensitivity was confirmed using a FRET technique. Lysosomal delivery of GemC18 by micelles was found to be critical for the cytotoxicity of the GemC18 because it was necessary for the GemC18 to be hydrolyzed by lysosomal enzymes to generate the active parent drug of gemcitabine. Most importantly, GemC18 carried by the pH-sensitive PHC micelles showed a significantly stronger *in vivo* antitumor activity than gemcitabine HCl in solution, GemC18 in solution, and GemC18 in the pH-insensitive PAC micelles, suggesting the acid-sensitive micelles as an effective delivery system for the lipophilized gemcitabine amide derivative, GemC18, and possibly the amide derivatives of other anticancer drugs.

## ASSOCIATED CONTENT

### Supporting Information

<sup>1</sup>H NMR and MS spectra of octadecanal; <sup>1</sup>H NMR and MALDI MS spectra of PEG2000-hydrazide; <sup>1</sup>H NMR and MALDI MS spectra of PEG2000-amine. This material is available free of charge via the Internet at <http://pubs.acs.org>.

## AUTHOR INFORMATION

### Corresponding Author

\*Tel.: +1 512 495 4758; fax: +1 512 471 7474. E-mail address: [zhengrong.cui@austin.utexas.edu](mailto:zhengrong.cui@austin.utexas.edu).

### Notes

The authors declare no competing financial interest.

## ACKNOWLEDGMENTS

This work was supported in part by a National Cancer Institute grant CA135274 (to Z.C.). We would like to thank Dr. Yue Li at the Microscopy Core Facility at the Dell Pediatric Research Institute at The University of Texas at Austin for assistance in acquiring the confocal microscopic images. The Fluorolog3 Fluorimeter was funded by the National Science Foundation Grant CHE-094750.

## REFERENCES

- (1) Matsumura, Y., and Maeda, H. (1986) A new concept for macromolecular therapeutics in cancer chemotherapy: mechanism of tumorotropic accumulation of proteins and the antitumor agent smancs. *Cancer Res.* 46, 6387–6392.
- (2) Iyer, A. K., Khaled, G., Fang, J., and Maeda, H. (2006) Exploiting the enhanced permeability and retention effect for tumor targeting. *Drug Discovery Today* 11, 812–818.
- (3) Kwon, G. S. (2003) Polymeric micelles for delivery of poorly water-soluble compounds. *Crit. Rev. Ther. Drug Carrier Syst.* 20, 357–403.
- (4) Otsuka, H., Nagasaki, Y., and Kataoka, K. (2003) PEGylated nanoparticles for biological and pharmaceutical applications. *Adv. Drug Delivery Rev.* 55, 403–419.

- (5) Torchilin, V. P. (2001) Structure and design of polymeric surfactant-based drug delivery systems. *J. Controlled Release* 73, 137–172.

- (6) Wang, Y., Wang, X., Zhang, Y., Yang, S., Wang, J., Zhang, X., and Zhang, Q. (2009) RGD-modified polymeric micelles as potential carriers for targeted delivery to integrin-overexpressing tumor vasculature and tumor cells. *J. Drug Targeting* 17, 459–467.

- (7) Nishiyama, N., and Kataoka, K. (2006) Current state, achievements, and future prospects of polymeric micelles as nano-carriers for drug and gene delivery. *Pharmacol. Ther.* 112, 630–648.

- (8) Huh, K. M., Lee, S. C., Cho, Y. W., Lee, J., Jeong, J. H., and Park, K. (2005) Hydrotropic polymer micelle system for delivery of paclitaxel. *J. Controlled Release* 101, 59–68.

- (9) Owens, D. E., 3rd., and Peppas, N. A. (2006) Opsonization, biodistribution, and pharmacokinetics of polymeric nanoparticles. *Int. J. Pharm.* 307, 93–102.

- (10) Rijcken, C. J., Soga, O., Hennink, W. E., and van Nostrum, C. F. (2007) Triggered destabilisation of polymeric micelles and vesicles by changing polymers polarity: an attractive tool for drug delivery. *J. Controlled Release* 120, 131–148.

- (11) Haag, R. (2004) Supramolecular drug-delivery systems based on polymeric core-shell architectures. *Angew. Chem., Int. Ed. Engl.* 43, 278–282.

- (12) Engin, K., Leeper, D. B., Cater, J. R., Thistlethwaite, A. J., Tupchong, L., and McFarlane, J. D. (1995) Extracellular pH distribution in human tumours. *Int. J. Hyperthermia* 11, 211–216.

- (13) Lee, E. S., Na, K., and Bae, Y. H. (2003) Polymeric micelle for tumor pH and folate-mediated targeting. *J. Controlled Release* 91, 103–113.

- (14) Boudier, A., Aubert-Pouëssel, A., Louis-Pence, P., Gérardin, C., Jorgensen, C., Devoisselle, J. M., and Bégu, S. (2009) The control of dendritic cell maturation by pH-sensitive polyion complex micelles. *Biomaterials* 30, 233–241.

- (15) Gillies, E. R., Jonsson, T. B., and Fréchet, J. M. (2004) Stimuli-responsive supramolecular assemblies of linear-dendritic copolymers. *J. Am. Chem. Soc.* 126, 11936–11943.

- (16) Toncheva, V., Schacht, E., Ng, S. Y., Barr, J., and Heller, J. (2003) Use of block copolymers of poly(ortho esters) and poly(ethylene glycol) micellar carriers as potential tumour targeting systems. *J. Drug Targeting* 11, 345–353.

- (17) Barton-Burke, M. (1999) Gemcitabine: a pharmacologic and clinical overview. *Cancer Nurs.* 22, 176–183.

- (18) Schmittl, A., Schuster, R., Bechrakis, N. E., Siehl, J. M., Foerster, M. H., Thiel, E., and Keilholz, U. (2005) A two-cohort phase II clinical trial of gemcitabine plus treosulfan in patients with metastatic uveal melanoma. *Melanoma Res.* 15, 447–451.

- (19) Corrie, P. G., Shaw, J., Spanswick, V. J., Sehmbi, R., Jonson, A., Mayer, A., Bulusu, R., Hartley, J. A., and Cree, I. A. (2005) Phase I trial combining gemcitabine and treosulfan in advanced cutaneous and uveal melanoma patients. *Br. J. Cancer* 92, 1997–2003.

- (20) Brusa, P., Immordino, M. L., Rocco, F., and Cattel, L. (2007) Antitumor activity and pharmacokinetics of liposomes containing lipophilic gemcitabine prodrugs. *Anticancer Res.* 27, 195–199.

- (21) Immordino, M. L., Brusa, P., Rocco, F., Arpicco, S., Ceruti, M., and Cattel, L. (2004) Preparation, characterization, cytotoxicity and pharmacokinetics of liposomes containing lipophilic gemcitabine prodrugs. *J. Controlled Release* 100, 331–346.

- (22) Celano, M., Calvagno, M. G., Bulotta, S., Paolino, D., Arturi, F., Rotiroli, D., Filetti, S., Fresta, M., and Russo, D. (2004) Cytotoxic effects of gemcitabine-loaded liposomes in human anaplastic thyroid carcinoma cells. *BMC Cancer* 4, 63.

- (23) Sloat, B. R., Sandoval, M. A., Li, D., Chung, W. G., Lansakara-P, D. S., Proteau, P. J., Kiguchi, K., DiGiovanni, J., and Cui, Z. (2011) *In vitro* and *in vivo* anti-tumor activities of a gemcitabine derivative carried by nanoparticles. *Int. J. Pharm.* 409, 278–288.

- (24) Reddy, L. H., Dubernet, C., Mouelhi, S. L., Marque, P. E., Desmaele, D., and Couvreur, P. (2007) A new nanomedicine of gemcitabine displays enhanced anticancer activity in sensitive and resistant leukemia types. *J. Controlled Release* 124, 20–27.

- (25) Arias, J. L., Reddy, L. H., and Couvreur, P. (2008) Magneto-responsive squalenoyl gemcitabine composite nanoparticles for cancer active targeting. *Langmuir* 24, 7512–7519.
- (26) Easton, C. J., Xia, L., Pitt, M. J., Ferrante, A., Poulos, A., and Rathjen, D. A. (2001) Polyunsaturated nitroalkanes and nitro-substituted fatty acids. *Synthesis* 3, 451–457.
- (27) Guo, Z., and Gallo, J. M. (1999) Selective protection of 2',2'-difluorodeoxycytidine (gemcitabine). *J. Org. Chem.* 64, 8319–8322.
- (28) Aguiar, J., Carpena, P., Molina-Bolívar, J. A., and Carnero Ruiz, C. (2003) On the determination of the critical micelle concentration by the pyrene 1:3 ratio method. *J. Colloid Interface Sci.* 258, 116–122.
- (29) MacLaughlin, F. C., Mumper, R. J., Wang, J., Tagliaferri, J. M., Gill, I., Hinchcliffe, M., and Rolland, A. P. (1998) Chitosan and depolymerized chitosan oligomers as condensing carriers for in vivo plasmid delivery. *J. Controlled Release* 56, 259–272.
- (30) Pasut, G., Canal, F., Dalla Via, L., Arpicco, S., Veronese, F. M., and Schiavon, O. (2008) Antitumoral activity of PEG-gemcitabine prodrugs targeted by folic acid. *J. Controlled Release* 127, 239–248.
- (31) Sethuraman, V. A., Lee, M. C., and Bae, Y. H. (2008) A biodegradable pH-sensitive micelle system for targeting acidic solid tumors. *Pharm. Res.* 25, 657–666.
- (32) Berney, C., and Danuser, G. (2003) FRET or no FRET: a quantitative comparison. *Biophys. J.* 84, 3992–4010.
- (33) Kim, S., Shi, Y., Kim, J. Y., Park, K., and Cheng, J. X. (2010) Overcoming the barriers in micellar drug delivery: loading efficiency, in vivo stability, and micelle-cell interaction. *Exp. Opin. Drug Delivery* 7, 49–62.
- (34) Aryal, S., Hu, C. M., and Zhang, L. (2010) Polymer-cisplatin conjugate nanoparticles for acid-responsive drug delivery. *ACS Nano* 4, 251–258.
- (35) Tang, R., Ji, W., Panus, D., Palumbo, R. N., and Wang, C. (2011) Block copolymer micelles with acid-labile ortho ester side-chains: Synthesis, characterization, and enhanced drug delivery to human glioma cells. *J. Controlled Release* 151, 18–27.
- (36) Lo, Y. L. (2003) Relationships between the hydrophilic-lipophilic balance values of pharmaceutical excipients and their multidrug resistance modulating effect in Caco-2 cells and rat intestines. *J. Controlled Release* 90, 37–48.
- (37) Kabanov, A. V., Batrakova, E. V., and Miller, D. W. (2003) Pluronic block copolymers as modulators of drug efflux transporter activity in the blood-brain barrier. *Adv. Drug Delivery Rev.* 55, 151–164.
- (38) <http://www.nc3rs.org.uk/bloodsamplingmicrosite/page.asp?id=419>
- (39) Kastantin, M., Ananthanarayanan, B., Karmali, P., Ruoslahti, E., and Tirrell, M. (2009) Effect of the lipid chain melting transition on the stability of DSPE-PEG(2000) micelles. *Langmuir* 25, 7279–7286.
- (40) Pandit, N. K. (2007) *Membranes and Tissues. Introduction to the Pharmaceutical Sciences* (Pandit, N. K., Eds.) pp 65, Lippincott Williams & Wilkins, Philadelphia.
- (41) Chen, H., Kim, S., He, W., Wang, H., Low, P. S., Park, K., and Cheng, J. X. (2008) Fast release of lipophilic agents from circulating PEG-PDLLA micelles revealed by in vivo forster resonance energy transfer imaging. *Langmuir* 24, 5213–5217.
- (42) Chen, H., Kim, S., Li, L., Wang, S., Park, K., and Cheng, J. X. (2008) Release of hydrophobic molecules from polymer micelles into cell membranes revealed by Forster resonance energy transfer imaging. *Proc. Natl. Acad. Sci. U. S. A.* 105, 6596–6601.
- (43) Xiao, L., Xiong, X., Sun, X., Zhu, Y., Yang, H., Chen, H., Gan, L., Xu, H., and Yang, X. (2011) Role of cellular uptake in the reversal of multidrug resistance by PEG-b-PLA polymeric micelles. *Biomaterials* 32, 5148–5157.
- (44) Kono, K., Kojima, C., Hayashi, N., Nishisaka, E., Kiura, K., Watarai, S., and Harada, A. (2008) Preparation and cytotoxic activity of poly(ethylene glycol)-modified poly(amidoamine) dendrimers bearing adriamycin. *Biomaterials* 29, 1664–1675.
- (45) Dosio, F., Brusa, P., Crosasso, P., Arpicco, S., and Cattel, L. (1997) Preparation, characterization and properties in vitro and in vivo of a paclitaxel–albumin conjugate. *J. Controlled Release* 47, 293–304.
- (46) Calvagno, M. G., Celia, C., Paolino, D., Cosco, D., Iannone, M., Castelli, F., Doldo, P., and Frest, M. (2007) Effects of lipid composition and preparation conditions on physical-chemical properties, technological parameters and in vitro biological activity of gemcitabine-loaded liposomes. *Curr. Drug Delivery* 4, 89–101.
- (47) Baldwin, S. A., Yao, S. Y., Hyde, R. J., Ng, A. M., Foppolo, S., Barnes, K., Ritzel, M. W., Cass, C. E., and Young, J. D. (2005) Functional characterization of novel human and mouse equilibrative nucleoside transporters (hENT3 and mENT3) located in intracellular membranes. *J. Biol. Chem.* 280, 15880–15887.